
Why Ask One When You Can Ask k ? Two-Stage Learning-to-Defer to a Set of Experts

Yannis Montreuil

School of Computing
National University of Singapore
Singapore, 118431, Singapore
yannis.montreuil@u.nus.edu

Axel Carlier

Institut de Recherche en Informatique de Toulouse
Institut national polytechnique de Toulouse
Toulouse, 31000, France
axel.carlier@toulouse-inp.fr

Lai Xing Ng

Institute for Infocomm Research
Agency for Science, Technology and Research
Singapore, 138632, Singapore
ng_lai_xing@i2r.a-star.edu.sg

Wei Tsang Ooi

School of Computing
National University of Singapore
Singapore, 118431, Singapore
ooiwt@comp.nus.edu.sg

Abstract

Learning-to-Defer (L2D) enables decision-making systems to improve reliability by selectively deferring uncertain predictions to more competent agents. However, most existing approaches focus exclusively on single-agent deferral, which is often inadequate in high-stakes scenarios that require collective expertise. We propose *Top- k Learning-to-Defer*, a generalization of the classical two-stage L2D framework that allocates each query to the k most confident agents instead of a single one. To further enhance flexibility and cost-efficiency, we introduce *Top- $k(x)$ Learning-to-Defer*, an adaptive extension that learns the optimal number of agents to consult for each query, based on input complexity, agent competency distributions, and consultation costs. For both settings, we derive a novel surrogate loss and prove that it is Bayes-consistent and $(\mathcal{R}, \mathcal{G})$ -consistent, ensuring convergence to the Bayes-optimal allocation. Notably, we show that the well-established model cascades paradigm arises as a restricted instance of our Top- k and Top- $k(x)$ formulations. Extensive experiments across diverse benchmarks demonstrate the effectiveness of our framework on both classification and regression tasks.

1 Introduction

Learning-to-Defer (L2D) is a principled framework for enhancing decision-making in high-stakes settings, where prediction errors can lead to significant consequences (Madras et al., 2018; Mozannar and Sontag, 2020; Verma et al., 2022). By leveraging a heterogeneous ensemble of agents—such as AI models, human experts, or other decision-makers—L2D learns to dynamically allocate each query to *the most competent agent*. In the *two-stage* variant (Narasimhan et al., 2022; Mao et al., 2023a), all agents are trained offline, and a separate allocation function is optimized to route each query to the agent with the highest expected utility. This setup is particularly valuable in domains like healthcare, where routine cases may be confidently handled by automated models, while ambiguous or anomalous inputs are deferred to human specialists (Mozannar et al., 2023). By design, L2D frameworks optimize both predictive performance and operational cost, making them well-suited for collaborative, safety-critical environments.

Despite their practical utility, existing Learning-to-Defer frameworks typically assume that each query is allocated to exactly one agent. While effective in controlled settings, this single-agent

deferral policy is often insufficient in complex, high-stakes scenarios where collective expertise is essential. Relying on a single decision-maker can result in incomplete assessments, heightened susceptibility to individual biases, and increased risk of errors or adversarial manipulation. In contrast, many real-world applications—such as cancer diagnosis, legal deliberation, and fraud detection—require aggregating insights from multiple experts to ensure robust, fair, and accountable outcomes. For instance, in oncology, multidisciplinary tumor boards composed of radiologists, pathologists, oncologists, and surgeons collaboratively evaluate patient cases to improve diagnostic accuracy and mitigate individual errors (Jiang et al., 1999; Fatima et al., 2017). Similar multi-agent decision processes arise in cybersecurity, judicial review, and financial risk assessment (Dietterich, 2000), underscoring the need for L2D frameworks that support deferral to multiple agents per query.

Motivated by these limitations, we extend the classical Two-Stage Learning-to-Defer framework to a novel *Top-k L2D* formulation, which allocates each query to the k most reliable agents, ranked by their predictive confidence. To further enhance flexibility and cost-efficiency, we introduce *Top-k(x) L2D*, an adaptive mechanism that learns the optimal number of agents to consult per query, based on input complexity, the distribution of agent competencies, and consultation costs. As a key theoretical insight, we show that classical model cascades (Viola and Jones, 2001; Saberian and Vasconcelos, 2014; Laskaridis et al., 2021; Dohan et al., 2022; Jitkrittum et al., 2024) arise as a restricted special case of both *Top-k* and *Top-k(x) L2D*—corresponding to fixed agent orderings, manually specified thresholds, and early stopping. By leveraging collective expertise, our framework significantly improves robustness, interpretability, and predictive performance in collaborative decision-making settings.

Our contributions are summarized as follows:

1. **Top-k L2D: Generalized Deferral to Multiple Agents.** We introduce *Top-k Learning-to-Defer*, a novel generalization of the classical Two-Stage L2D framework that allocates each query to a set of the top- k most reliable agents (Section 4.1). This design overcomes the limitations of single-agent deferral by enabling collaborative, expert-aggregated decision-making.
2. **Rigorous Theoretical Guarantees.** We derive a new surrogate loss and prove that it is both Bayes-consistent and $(\mathcal{R}, \mathcal{G})$ -consistent, ensuring convergence toward the Bayes-optimal top- k deferral policy (Section 4.3).
3. **Top-k(x) L2D: Adaptive Agent Selection.** We propose *Top-k(x) Learning-to-Defer*, an adaptive extension that learns the optimal number of agents to consult per query by jointly accounting for input complexity, agent competencies, and consultation costs (Section 4.4).
4. **Model Cascades as a Special Case.** As a key theoretical insight, we show that the classical model cascades paradigm arises as a special case of both *Top-k* and *Top-k(x) L2D*, positioning our framework as a strict generalization of existing approaches. See Sections A.4 and A.5.
5. **Extensive Empirical Validation.** We empirically validate our framework on diverse classification and regression benchmarks, where both *Top-k* and *Top-k(x) L2D* consistently outperform competitive baselines (Section 5).

2 Related Work

Learning-to-Defer (Madras et al., 2018; Mozannar and Sontag, 2020; Verma et al., 2022) extends the Learning-from-Abstention framework (Chow, 1970; Bartlett and Wegkamp, 2008; Geifman and El-Yaniv, 2017; Cortes et al., 2016), wherein queries are assigned to the most suitable agents instead of outright rejection. Our focus lies specifically on the *two-stage* variant of Learning-to-Defer, which involves offline training of all agents and learning a dedicated function for optimal query allocation.

Two-Stage Learning-to-Defer. The two-stage Learning-to-Defer framework, introduced by Narasimhan et al. (2022); Mao et al. (2023a), comprises a primary model and multiple experts trained offline. An independent function, the *rejector*, is subsequently learned to route queries to the most appropriate agent. Recent extensions of this paradigm include regression-focused models (Mao et al., 2024), multi-task settings (Montreuil et al., 2024), robustness (Montreuil et al., 2025a), and diverse applications (Palomba et al., 2025; Montreuil et al., 2025b; Strong et al., 2024).

Consistency in Top- k Classification. Top- k classification generalizes standard classification by predicting a set of the most probable classes rather than a single class. Early research introduced top- k hinge loss variants (Lapin et al., 2015, 2016b), which were later shown to lack Bayes consistency (Yang and Koyejo, 2020). Alternative non-convex approaches encountered practical optimization challenges (Yang and Koyejo, 2020; Thilagar et al., 2022). Recent advances by Cortes et al. (2024) have established the Bayes-consistency and \mathcal{H} -consistency of several surrogate losses, including cross-entropy (Mao et al., 2023b) and constrained losses (Cortes and Vapnik, 1995), significantly enhancing the theoretical understanding of top- k classification.

Our Contribution. We bridge two-stage Learning-to-Defer and top- k classification by proposing a novel framework that allows deferral to multiple experts simultaneously, rather than relying on a single agent. To our knowledge, this intersection has not been previously explored, marking our work as the first to unify these two research directions.

3 Preliminaries

Two-Stage Learning-to-Defer. Let \mathcal{X} be the input space and let \mathcal{Z} denote an arbitrary¹ output space. Each example $(x, z) \in \mathcal{X} \times \mathcal{Z}$ is drawn i.i.d. from an unknown distribution \mathcal{D} . We consider the hypothesis class $\mathcal{G} = \{g : \mathcal{X} \rightarrow \mathcal{Z}\}$ with predictions defined as $g(x) \in \mathcal{Z}$. When \mathcal{Z} is finite, g can be instantiated via a scoring function $q : \mathcal{X} \times \mathcal{Z} \rightarrow \mathbb{R}$ with $g(x) = \arg \max_{z \in \mathcal{Z}} q(x, z)$; when \mathcal{Z} is continuous, g may be any measurable map into \mathcal{Z} .

The Learning-to-Defer (L2D) framework allocates a query $x \in \mathcal{X}$ to the most suitable *agent*, leveraging their respective competencies to enhance predictive performance (Madras et al., 2018; Mozannar and Sontag, 2020; Verma et al., 2022). Agents consist of a main model g and a set of J experts. Formally, the *set of agents* is defined as $a = \{g, m_1, \dots, m_J\}$ and the *set of indexed agents* by $\mathcal{A} = \{0\} \cup [J]$, where agent 0 corresponds to the main model a_0 (or g), and each expert $j \in [J]$ is represented by a_j (or m_j). The prediction of each agent a_j is given by

$$a_j(x) = \begin{cases} g(x), & j = 0 \quad (\text{main model}), \\ m_j(x), & j > 0 \quad (\text{expert } j), \end{cases}$$

with expert predictions $m_j(x) \in \mathcal{Z}$. In the two-stage setting, all agents are trained offline, we fully have access to the main model g , and experts m_j are available on demand (Mao et al., 2023a, 2024; Montreuil et al., 2024, 2025b,a).

We introduce a rejector function $r \in \mathcal{R}$, defined as $r : \mathcal{X} \rightarrow \mathcal{A}$, which assigns each query x to an agent based on the highest rejection score $r(x) = \arg \max_{j \in \mathcal{A}} r(x, j)$. This rejector is trained by minimizing appropriate losses, formally defined as follows:

Definition 3.1 (Two-Stage L2D Losses). Let an input $x \in \mathcal{X}$, rejector $r \in \mathcal{R}$, and the agent set a . The *true deferral loss* ℓ_{def} and its convex, non-negative, upper-bound surrogate deferral losses Φ_{def}^u are defined as

$$\ell_{\text{def}}(r(x), a(x), z) = \sum_{j=0}^J c_j(a_j(x), z) 1_{r(x)=j}, \quad \Phi_{\text{def}}^u(r, a, x, z) = \sum_{j=0}^J \tau_j(a(x), z) \Phi_{01}^u(r, x, j),$$

where $c_j(a_j(x), z) \geq 0$ denotes the bounded cost of assigning the query x to agent j (Madras et al., 2018), and $\tau_j(a(x), z) = \sum_{i \neq j} c_i(a_i(x), z)$ aggregates the costs from all other agents. Specifically, assigning the query to an agent j incurs a cost $c_j(a_j(x), z) = \alpha_j \psi(a_j(x), z) + \beta_j$. Here, $\psi : \mathcal{Z} \times \mathcal{Z} \rightarrow \mathbb{R}_+$ quantifies prediction quality, β_j represents a consultation cost, and α_j is a scaling factor.

Remark 1. In classification, the function ψ corresponds to the 0-1 loss. The special case $\alpha_j = 0$ corresponds to the learning-with-abstention scenario (Bartlett and Wegkamp, 2008; Cortes et al., 2016).

¹Typical choices are $\mathcal{Z} = \mathcal{Y}$ with $\mathcal{Y} = \{1, \dots, n\}$ for multi-class classification, or $\mathcal{Z} = \mathcal{T} \subseteq \mathbb{R}$ for regression, but the theory does not require any special structure on \mathcal{Z} .

Top- k Classification. Consider a multiclass classification setting, where each input $x \in \mathcal{X}$ is assigned one of $|\mathcal{Y}|$ possible labels $y \in \mathcal{Y}$ (Lapin et al., 2016b; Yang and Koyejo, 2020). Given an integer $k \leq |\mathcal{Y}|$, we define the *prediction set* $H_k(x)$ as the set containing the k labels with the highest scores according to $h(x, \cdot)$. Specifically, let the labels be ordered such that $h(x, h_{[1]_h^\downarrow}(x)) \geq h(x, h_{[2]_h^\downarrow}(x)) \geq \dots \geq h(x, h_{[k]_h^\downarrow}(x))$, where the subscript notation $[i]_h^\downarrow$ indicates that the ordering is induced by the descending values of $h(x, \cdot)$. We formally define this permutation notation in Appendix A.1. Accordingly, we introduce

$$H_k(x) = \{h_{[1]_h^\downarrow}(x), h_{[2]_h^\downarrow}(x), \dots, h_{[k]_h^\downarrow}(x)\} = \{[1]_h^\downarrow, [2]_h^\downarrow, \dots, [k]_h^\downarrow\}. \quad (1)$$

When $k = 1$, we recover the standard single-label prediction $h_{[1]_h^\downarrow}(x) = \arg \max_{y \in \mathcal{Y}} h(x, y)$. Conversely, setting $k = |\mathcal{Y}|$ yields the entire label set \mathcal{Y} . To quantify prediction errors, the usual 0-1 loss is extended to the *top- k loss*, defined as $\ell_k(H_k(x), y) = \mathbb{1}_{y \notin H_k(x)}$.

The top- k loss ℓ_k is discontinuous with respect to the scores $\{h(x, y) : y \in \mathcal{Y}\}$, rendering direct optimization computationally infeasible (Lapin et al., 2016a,b; Yang and Koyejo, 2020; Thilagar et al., 2022; Cortes et al., 2024). Therefore, practical training methods rely on differentiable surrogate losses, which approximate ℓ_k and enable gradient-based optimization (Zhang, 2002; Steinwart, 2007; Bartlett et al., 2006).

Top- k Consistency The main objective is to identify a classifier $h \in \mathcal{H}$ that minimizes the true top- k error $\mathcal{E}_{\ell_k}(h)$, defined as $\mathcal{E}_{\ell_k}(h) = \mathbb{E}_{(x,y)}[\ell_k(H_k(x), y)]$. The Bayes-optimal error is expressed as $\mathcal{E}_{\ell_k}^B(\mathcal{H}) = \inf_{h \in \mathcal{H}} \mathcal{E}_{\ell_k}(h)$. However, minimizing $\mathcal{E}_{\ell_k}(h)$ directly is challenging due to the non-differentiability of the *true multiclass 0-1 loss* (Zhang, 2002; Steinwart, 2007; Awasthi et al., 2022) and by extension, the top- k loss (Lapin et al., 2016a,b; Yang and Koyejo, 2020; Thilagar et al., 2022; Cortes et al., 2024). To address this challenge, surrogate losses are employed as convex, non-negative upper bounds on ℓ_k . A notable family of multiclass surrogates is the comp-sum (Mohri et al., 2012; Mao et al., 2023b; Wang and Scott, 2023), defined as:

$$\Phi_{01}^u(h, x, y) = \Psi^u \left(\sum_{y' \neq y} \Psi_e(h(x, y) - h(x, y')) \right), \quad (2)$$

where $\Psi_e(v) = \exp(-v)$, which defines the cross-entropy family. For $u > 0$, the transformation is given by:

$$\Psi^u(v) = \begin{cases} \log(1 + v) & \text{if } u = 1, \\ \frac{1}{1-u} [(1 - v)^{1-u} - 1] & \text{if } u > 0 \wedge u \neq 1. \end{cases} \quad (3)$$

This formulation generalizes several well-known loss functions, including the sum-exponential loss (Weston and Watkins, 1998), logistic loss (Ohn Aldrich, 1997), generalized cross-entropy (Zhang and Sabuncu, 2018), and mean absolute error loss (Ghosh et al., 2017). The corresponding true error for Φ_{01}^u is defined as $\mathcal{E}_{\Phi_{01}^u}(h) = \mathbb{E}_{(x,y)}[\Phi_{01}^u(h, x, y)]$, with its optimal value expressed as $\mathcal{E}_{\Phi_{01}^u}^*(\mathcal{H}) = \inf_{h \in \mathcal{H}} \mathcal{E}_{\Phi_{01}^u}(h)$. A key property of a surrogate loss is the *consistency*, which ensures that minimizing the surrogate excess risk leads to minimizing the true excess risk (Zhang, 2002; Bartlett et al., 2006; Steinwart, 2007; Tewari and Bartlett, 2007). To characterize consistency with a particular hypothesis set \mathcal{H} , Awasthi et al. (2022) introduced \mathcal{H} -consistency bounds.

Theorem 3.2 (\mathcal{H} -consistency bounds). *The surrogate Φ_{01}^u is \mathcal{H} -consistent with respect to ℓ_k if there exists a non-decreasing function $\Gamma : \mathbb{R}^+ \rightarrow \mathbb{R}^+$ such that for any distribution \mathcal{D} , the following holds,*

$$\mathcal{E}_{\ell_k}(h) - \mathcal{E}_{\ell_k}^B(\mathcal{H}) + \mathcal{U}_{\ell_k}(\mathcal{H}) \leq \Gamma \left(\mathcal{E}_{\Phi_{01}^u}(h) - \mathcal{E}_{\Phi_{01}^u}^*(\mathcal{H}) + \mathcal{U}_{\Phi_{01}^u}(\mathcal{H}) \right),$$

where the minimizability gap $\mathcal{U}_{\ell_{01}}(\mathcal{H})$ quantifies the difference between the best-in-class excess risk and the expected pointwise minimum error: $\mathcal{U}_{\ell_{01}}(\mathcal{H}) = \mathcal{E}_{\ell_k}^B(\mathcal{H}) - \mathbb{E}_x [\inf_{h \in \mathcal{H}} \mathbb{E}_{y|x} [\ell_k(H_k(x), y)]]$. The gap vanishes when $\mathcal{H} = \mathcal{H}_{\text{all}}$ and recovers Bayes-consistency by taking the asymptotic limit (Zhang, 2002; Steinwart, 2007; Bartlett et al., 2006; Awasthi et al., 2022).

4 Top- k Learning-to-Defer

Motivation. Existing Two-Stage Learning-to-Defer (L2D) frameworks (Mao et al., 2023a, 2024; Montreuil et al., 2024, 2025a,b) predominantly focus on selecting a single most suitable agent to

handle each query x . While theoretically grounded, this one-to-one allocation can be limiting in scenarios marked by uncertainty, high complexity, or elevated decision risk. For instance, in critical medical applications such as cancer diagnosis, deferring a decision to a single agent—as done in classical Learning-to-Defer settings (Madras et al., 2018)—may raise ethical concerns and introduce potential vulnerabilities. In practice, decisions in such settings often demand the involvement or consensus of multiple experts to ensure robustness, fairness, and accountability.

To address these limitations, we propose a novel approach in which each query is allocated to a *set* of the k most suitable agents. In the following, we introduce our method for learning to allocate each query to the top- k agents based on their deferral scores.

4.1 Introducing the Top- k Learning-to-Defer Problem

In standard Two-Stage Learning-to-Defer, a rejector $r \in \mathcal{R}$ assigns each query $x \in \mathcal{X}$ to exactly one agent by minimizing the deferral loss ℓ_{def} introduced in Definition 3.1. We generalize the single-agent selection to the selection of the top- k agents through a novel construct: the *rejector set*.

Definition 4.1 (Rejector Set). Given a query $x \in \mathcal{X}$, a rejector function $r \in \mathcal{R}$ assigns a rejection score $r(x, j)$ to each agent $j \in \mathcal{A}$. For the number of queried agents $k \leq |\mathcal{A}|$, the *rejector set* $R_k(x)$ consists of the indices of the top- k agents ranked by these scores:

$$R_k(x) = \{r_{[0]_r^\downarrow}(x), r_{[1]_r^\downarrow}(x), \dots, r_{[k-1]_r^\downarrow}(x)\} = \{[0]_r^\downarrow, [1]_r^\downarrow, \dots, [k-1]_r^\downarrow\},$$

where the indices satisfy the ordering

$$r(x, r_{[0]_r^\downarrow}(x)) \geq r(x, r_{[1]_r^\downarrow}(x)) \geq \dots \geq r(x, r_{[k-1]_r^\downarrow}(x)).$$

Here, k denotes the number of agents selected to make a prediction but also the cardinality of the rejector set. The agent with the highest rejection score is given by $r_{[0]_r^\downarrow}(x) = \arg \max_{j \in \mathcal{A}} r(x, j)$, where $r(x, j)$ denotes the score assigned to agent j . More generally, $r_{[k-1]_r^\downarrow}(x)$ refers to the agent ranked k -th in descending order of these scores, according to the ordering induced by $r(x, \cdot)$.

Using the rejector set, we adapt the single-agent deferral loss to define the *top- k deferral loss*, designed explicitly for scenarios involving multiple selected agents:

Lemma 4.2 (Top- k Deferral Loss). Let $x \in \mathcal{X}$ be a query and $R_k(x) \subseteq \mathcal{A}$ the rejector set from Definition 4.1. The top- k deferral loss is defined as:

$$\ell_{\text{def},k}(R_k(x), a(x), x, z) = \sum_{j=0}^J c_j(a_j(x), z) \mathbf{1}_{j \in R_k(x)}.$$

The proof of Lemma 4.2 is provided in Appendix A.6. Intuitively, this loss aggregates the individual costs $c_j(a_j(x), z)$ associated with each agent in the rejector set $R_k(x)$. For instance, consider a scenario with three agents $\mathcal{A} = \{0, 1, 2\}$ and a rejector set $R_2(x) = \{2, 1\}$. Here, the top-2 deferral loss explicitly computes the combined cost $c_2(m_2(x), z) + c_1(m_1(x), z)$, reflecting that both agents 2 and 1 handle the query x , with agent 2 having the highest rejector score.

Remark 2. Setting $k = 1$ reduces to the single-agent selection scenario, recovering the standard deferral loss introduced in Definition 3.1.

Remark 3. In Lemma A.4, we formally show that our *Top- k Learning-to-Defer* framework strictly generalizes classical model cascades (Viola and Jones, 2001; Saberian and Vasconcelos, 2014; Dohan et al., 2022; Jitkrittum et al., 2024), which arise as a weaker case when the agent ordering is fixed for all inputs, threshold values are manually specified, and inference stops at the first agent exceeding its confidence threshold. The generalisation is strict: Top- k L2D can (i) consult several non-contiguous experts simultaneously, (ii) learn an input-dependent number of experts with consistency guarantees, and (iii) aggregate their outputs, none of which is possible in classical sequential cascades.

4.2 Top- k L2D: Introducing the Surrogate for the Top- k Deferral Loss

Similar to the top- k classification setting, we require a surrogate loss to approximate the novel top- k deferral loss introduced in Lemma 4.4. To establish this surrogate, we utilize the comp-sum family of surrogate losses Φ_{01}^u defined in Section 3. These surrogates provide convex, non-negative upper bounds for the top- k loss ℓ_k (Yang and Koyejo, 2020; Cortes et al., 2024). Leveraging these properties, we first formalized an explicit upper bound on the top- k deferral loss.

Lemma 4.3 (Upper-Bounding the Top- k Deferral Loss). *Let $x \in \mathcal{X}$ be an input, and $k \leq |\mathcal{A}|$ the size of the rejector set. Then, the top- k deferral loss satisfies:*

$$\ell_{def,k}(R_k(x), a(x), x, z) \leq \sum_{j=0}^J \tau_j(a(x), z) \Phi_{01}^u(r, x, j) - (J - k) \sum_{j=0}^J c_j(a_j(x), z).$$

The detailed proof is provided in Appendix A.7. Setting $k = 1$ recovers the formulation from prior works established in Mao et al. (2024); Montreuil et al. (2024). This bound explicitly highlights the relationship between the top- k deferral loss, the cardinality k , and the number of experts J . Crucially, the second term of the upper bound does not depend on the rejector function $r \in \mathcal{R}$. This observation allows us to define a surrogate independent of these parameters, as shown in Appendix A.8.

Corollary 4.4 (Surrogate for the Top- k Deferral Loss). *Let $x \in \mathcal{X}$ be an input. The surrogate for the top- k deferral loss is defined as*

$$\Phi_{def,k}^u(r, a, x, z) = \sum_{j=0}^J \tau_j(a(x), z) \Phi_{01}^u(r, x, j),$$

whose minimization is notably independent of the cardinality parameter k .

This surrogate does not depend on the specific choice of rejector set $R_k(x)$ or its cardinality k . Therefore, training separate rejectors for different values of k is unnecessary, making this surrogate both computationally efficient and versatile. Importantly, this surrogate is exactly the same as the single-expert allocation case presented in Definition 3.1.

Although $\Phi_{def,k}^u$ is a convex, non-negative surrogate that upper-bounds the top- k deferral loss and is independent of k , these properties alone do not guarantee that minimizing it yields an optimal rejector set $R_k(x)$. To address this, we first formalize the Bayes-optimal rejector set $R_k^B(x)$ in the next subsection. We then provide a rigorous consistency analysis, proving that minimizing $\Phi_{def,k}^u$ is both Bayes-consistent and $(\mathcal{R}, \mathcal{G})$ -consistent. This ensures that the learned rejector set $R_k(x)$ asymptotically approximates the Bayes-optimal solution $R_k^B(x)$.

4.3 Theoretical Guarantees

4.3.1 Optimality of the Rejector Set

We begin by analyzing the optimal selection of agents within the rejector set $R_k(x)$. In the standard Two-Stage L2D framework, the Bayes-optimal rejector $r^B(x)$ assigns each query to the agent minimizing the expected cost according to the Bayes-optimal rule $r^B(x) = \arg \min_{j \in \mathcal{A}} \bar{c}_j^*(a_j(x), z)$, where $\bar{c}_0^*(a_0(x), z) = \inf_{g \in \mathcal{G}} \mathbb{E}_{z|x}[c_0(g(x), z)]$ and $\bar{c}_{j>0}^*(a_j(x), z) = \mathbb{E}_{z|x}[c_j(m_j(x), z)]$, as established by Narasimhan et al. (2022); Mao et al. (2023a, 2024); Montreuil et al. (2024).

In contrast, our proposed Top- k L2D framework generalizes the Bayes-optimal rule by allocating each query to a ranked set of the top- k agents, thereby yielding a more expressive and flexible allocation policy.

Lemma 4.5 (Bayes-optimal Rejector Set). *For a given query $x \in \mathcal{X}$, the Bayes-optimal rejector set $R_k^B(x)$ is defined as the subset of k agents with the lowest expected costs, ordered in increasing cost:*

$$R_k^B(x) = \arg \min_{\substack{R_k(x) \subseteq \mathcal{A} \\ |R_k(x)|=k}} \sum_{j \in R_k(x)} \bar{c}_j^*(a_j(x), z) = \{[0]_{\bar{c}^*}^\uparrow, [1]_{\bar{c}^*}^\uparrow, \dots, [k-1]_{\bar{c}^*}^\uparrow\},$$

where the ordering within $R_k^B(x)$ satisfies:

$$\forall j, j' \in R_k^B(x), \quad j < j' \implies \bar{c}_j^*(a_j(x), z) \leq \bar{c}_{j'}^*(a_{j'}(x), z).$$

The proof of Lemma 4.5 is provided in Appendix A.9. This Bayes-optimal selection policy identifies the k most suitable agents by minimizing their expected costs, thereby generalizing prior formulations from Narasimhan et al. (2022); Mao et al. (2023a, 2024); Montreuil et al. (2024). It provides a principled characterization of optimal multi-agent allocations in Learning-to-Defer settings.

Next, we demonstrate that the Bayes-optimal rejector set can be efficiently approximated through minimization of the surrogate top- k deferral loss.

4.3.2 Consistency of Top- k Deferral Surrogates

Our goal is to approximate the Bayes-optimal rejector set $R_k^B(x)$ by a learned rejector set $R_k^*(x)$ minimizing the surrogate introduced in Corollary 4.4. The Bayes-optimal set $R_k^B(x)$ minimizes the expected risk associated with the top- k deferral loss. Establishing the consistency of surrogate losses guarantees that minimizing them asymptotically recovers the Bayes-optimal deferral strategy proven in Lemma 4.5. Recent work by Cortes et al. (2024) established that the comp-sum family of surrogates Φ_{01}^u is both Bayes-consistent and \mathcal{H} -consistent with respect to the top- k loss ℓ_k for a classifier $h \in \mathcal{H}$. However, the consistency of surrogates specifically designed for the top- k deferral loss remains open and requires rigorous theoretical examination.

To address this gap, we focus on hypothesis classes \mathcal{R} that are *regular for top- k classification*, meaning that the rejector set $R_{|\mathcal{A}|}(x)$ consists of distinct elements covering all outcomes of \mathcal{A} . This assumption is mild in practice, as standard hypothesis sets, such as \mathcal{R}_{lin} and \mathcal{R}_{all} , satisfy regularity for top- k classification. Additionally, we assume that \mathcal{R} is *symmetric and complete*. Symmetry implies that \mathcal{R} is invariant under permutations of agent indices $j \in \mathcal{A}$, reflecting the fact that the ordering of agents is irrelevant in Learning-to-Defer settings. Completeness ensures that the rejector scores $r(x, j)$ can take arbitrary real values, i.e., they span \mathbb{R} .

Under these mild assumptions, we present the following consistency theorem, proven in Appendix A.10:

Theorem 4.6 ((\mathcal{G}, \mathcal{R})-Consistency Bound). *Let $x \in \mathcal{X}$, and consider a hypothesis class \mathcal{R} that is regular, complete, and symmetric, along with any distribution \mathcal{D} . Suppose the comp-sum surrogate family is \mathcal{R} -consistent. Then, there exists a non-decreasing, non-negative, concave function $\tilde{\Gamma}^u : \mathbb{R}^+ \rightarrow \mathbb{R}^+$, associated with the top- k loss ℓ_k and any surrogate from the comp-sum family parameterized with u , such that the following bound holds:*

$$\begin{aligned} \mathcal{E}_{\ell_{\text{def},k}}(g, r) - \mathcal{E}_{\ell_{\text{def},k}}^B(\mathcal{G}, \mathcal{R}) - \mathcal{U}_{\ell_{\text{def},k}}(\mathcal{G}, \mathcal{R}) &\leq \tilde{\Gamma}^u \left(\mathcal{E}_{\Phi_{\text{def},k}^u}(r) - \mathcal{E}_{\Phi_{\text{def},k}^u}^*(\mathcal{R}) - \mathcal{U}_{\Phi_{\text{def},k}^u}(\mathcal{R}) \right) \\ &\quad + \mathbb{E}_x \left[\bar{c}_0(g(x), z) - \inf_{g \in \mathcal{G}} \bar{c}_0(g(x), z) \right], \end{aligned}$$

where $\bar{c}_0(g(x), z) = \mathbb{E}_{z|x}[c_0(g(x), z)]$, $Q = \sum_{j=0}^J \mathbb{E}_{z|x}[\tau_j(a(x), z)]$, and $\tilde{\Gamma}^u(v) = Q\Gamma^u\left(\frac{v}{Q}\right)$.

Theorem 4.6 establishes a consistency bound linking the excess risk under the top- k deferral loss $\ell_{\text{def},k}$ to the excess risk under its surrogate $\Phi_{\text{def},k}^u$. The bound indicates that minimizing the surrogate effectively minimizes the original top- k deferral loss, ensuring the learned rejector set $R_k^*(x)$ approximates the Bayes-optimal rejector set $R_k^B(x)$. If the main model g is near-optimal after offline training, we have $\mathbb{E}_x[\bar{c}_0(g(x), z) - \inf_{g \in \mathcal{G}} \bar{c}_0(g(x), z)] \leq \epsilon$. Furthermore, suppose the surrogate risk satisfies $\mathcal{E}_{\Phi_{\text{def},k}^u}(r) - \mathcal{E}_{\Phi_{\text{def},k}^u}^*(\mathcal{R}) - \mathcal{U}_{\Phi_{\text{def},k}^u}(\mathcal{R}) \leq \epsilon_1$. Then, it follows that:

$$\mathcal{E}_{\ell_{\text{def},k}}(g, r) - \mathcal{E}_{\ell_{\text{def},k}}^B(\mathcal{G}, \mathcal{R}) - \mathcal{U}_{\ell_{\text{def},k}}(\mathcal{G}, \mathcal{R}) \leq \tilde{\Gamma}^u(\epsilon_1) + \epsilon,$$

confirming the surrogate’s effectiveness in approximating the Bayes-optimal rejector set from Lemma 4.5.

Remark 4. The minimizability gaps vanish under realizable distributions when $\mathcal{R} = \mathcal{R}_{\text{all}}$ and $\mathcal{G} = \mathcal{G}_{\text{all}}$. Moreover, by setting $\mathcal{R} = \mathcal{R}_{\text{all}}$ and $\mathcal{G} = \mathcal{G}_{\text{all}}$ and analyzing the asymptotic behavior in Theorem 4.6, we recover the classical notion of Bayes consistency (Zhang, 2002; Bartlett et al., 2006; Zhang and Agarwal, 2020).

4.4 Top- $k(x)$ L2D: Selecting the Optimal Number of Agents $k(x)$ Per Query

Motivation. While previous sections established that our surrogate losses are both (\mathcal{G}, \mathcal{R})-consistent and Bayes-consistent—ensuring that we asymptotically recover the Bayes-optimal rejector set $R_k^B(x)$ —it remains equally important to determine the optimal number of agents k necessary for reliable predictions. Instead of setting k as a global constant, we propose dynamically adapting k to each query as a function $k(x)$, tailored to the intrinsic complexity of query x and the underlying distribution of agents’ competencies.

Traditional Top- k L2D methods require predefining a fixed number of agents for all queries, leading to an expected cardinality of $\mathbb{E}_x[|R_k(x)|] = k$. By contrast, our adaptive approach can potentially

reduce the expected number of agents consulted per query $\mathbb{E}_x[|R_{k(x)}(x)|] = \mathbb{E}_x[k(x)] \leq \mathbb{E}_x[|R_k(x)|]$ for the same performance.

Choosing a larger k can enhance decision reliability by aggregating diverse expert opinions; however, it also incurs higher consultation costs and increases the risk of including less competent or erroneous agents. Conversely, a smaller k reduces computational and monetary costs but may lead to compromised prediction accuracy, particularly in complex or uncertain scenarios. To address this trade-off effectively, we introduce an adaptive strategy that learns the optimal cardinality by jointly considering the relative competencies of the available agents and the inherent difficulty of each input query.

Formulation. To address the adaptive selection of the number of agents, we build upon the framework recently introduced by Cortes et al. (2024). Our objective is to minimize the cardinality of a previously learned full rejector set $\hat{R}_{|\mathcal{A}|}(x)$, while preserving high decision accuracy. To this end, we introduce a *selector function* $s : \mathcal{X} \rightarrow \mathcal{A}$, drawn from a hypothesis class \mathcal{S} , which maps an input x to an index indicating the number of agents to retain. Specifically, the adaptive number of agents is given by $k(x) = s(x) + 1$, where $s(x) = \arg \max_{i \in \mathcal{A}} s(x, i)$. The corresponding top- $k(x)$ agents are then selected from the ordered rejector set $\hat{R}_{k(x)}(x)$, which is constructed using the learned rejector $\hat{r} \in \mathcal{R}$.

The selector function is learned by minimizing the following *cardinality loss* for L2D:

Definition 4.7 (Cardinality Loss for L2D). Let $x \in \mathcal{X}$, a learned rejector set $\hat{R}_{|\mathcal{A}|}(x)$, a chosen metric $d : \mathcal{X} \rightarrow \mathbb{R}^+$, an increasing non-negative function ξ , and a hyperparameter $\lambda \geq 0$. The cardinality loss tailored to our problem is defined as:

$$\ell_{\text{car}}(\hat{R}_{s(x)+1}(x), s(x), a(x), z) = d(\hat{R}_{s(x)+1}(x), s(x), a(x), z) + \lambda \xi \left(\sum_{i=0}^{s(x)} \beta_{[i]_{\hat{r}}} \right),$$

using the normalized loss $\tilde{\ell}_{\text{car}}$ leads to the surrogate defined as:

$$\Phi_{\text{car}}(\hat{R}_{|\mathcal{A}|}(x), s, a(x), z) = \sum_{v \in \mathcal{A}} (1 - \tilde{\ell}_{\text{car}}(\hat{R}_{v+1}(x), v, a(x), z)) \Phi_{01}^u(s, x, v),$$

The term $d(\hat{R}_{s(x)+1}(x), s(x), a(x), z)$ quantifies the prediction error incurred by the selected rejector set. Common metrics include the top- k loss, 0-1 loss under majority voting, and weighted majority voting, depending on the task. We provide additional examples of this metric in Appendix A.12, covering both classification and regression settings. In parallel, the regularization term $\lambda \xi \left(\sum_{i=0}^{s(x)} \beta_{[i]_{\hat{r}}} \right)$ penalizes the unnecessary use of agents that incur consultation costs. Here, ξ is a monotonic function, and $\beta_{[i]_{\hat{r}}}$ denotes the cost associated with the agent ranked i -th by the learned rejector \hat{r} .

Cortes et al. (2024) have demonstrated that the cardinality loss ℓ_{car} can be effectively minimized using comp-sum surrogates Φ_{01}^u , guaranteeing \mathcal{S} -consistency. Leveraging this consistency along with the Bayes-optimal rejector set structure (Lemma 4.5), we obtain the following key result:

Lemma 4.8 (Bayes-Optimal Rejector Set with Bayes-Optimal Cardinality). *Let $x \in \mathcal{X}$ and the learned rejector set $\hat{R}_k(x)$. Define the optimal cardinality as:*

$$s^B(x) = \arg \min_{v \in \mathcal{A}} \mathbb{E}_{z|x} \left[\ell_{\text{car}} \left(\hat{R}_{v+1}(x), v, a(x), z \right) \right],$$

where $\hat{R}_{v+1}(x)$ is a rejector set of size $v + 1$. Then, the Bayes-optimal rejector set $\hat{R}_{s^B(x)+1}(x)$ selects exactly the $s^B(x) + 1$ agents with the lowest Bayes-optimal expected costs:

$$\hat{R}_{s^B(x)+1}(x) = \hat{R}_k(x) \Big|_{k=s^B(x)+1}.$$

Lemma 4.8, proven in Appendix A.11, implies that learning the Bayes-optimal cardinality yields the most cost-effective minimal rejector set. Due to established consistency results, our learned rejector set $\hat{R}_{s^*(x)+1}(x)$ with optimal number of agents $s^*(x) + 1$, effectively approximates the Bayes-optimal solution $\hat{R}_{s^B(x)+1}(x)$.

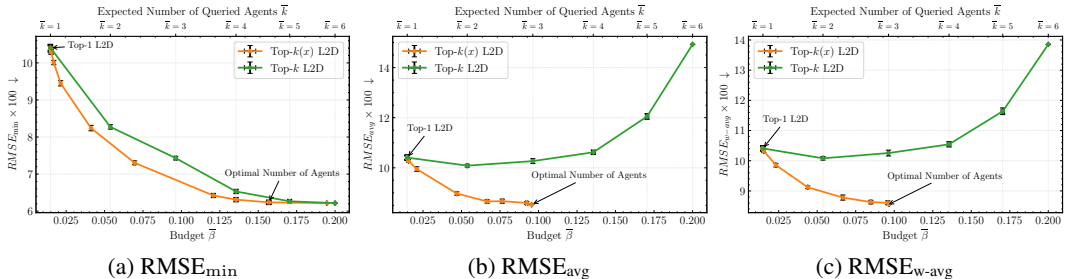
Remark 5. In Lemma A.6, we formally show that our *Top- $k(x)$ Learning-to-Defer* framework strictly generalizes classical model cascades.

5 Experiments

We evaluate the performance of our proposed methods—*Top-k L2D* and its adaptive extension *Top-k(x) L2D*—against state-of-the-art baselines from the Two-Stage Learning-to-Defer literature (Mao et al., 2023a, 2024). Our experiments span both classification tasks, including CIFAR-100 (Krizhevsky, 2009) and SVHN (Goodfellow et al., 2014), as well as a regression task on the California Housing dataset (Kelley Pace and Barry, 1997). In all settings, *Top-k* and *Top-k(x) L2D* consistently outperform single-agent deferral methods (Mao et al., 2023a, 2024).

We present detailed results across multiple evaluation metrics on the California Housing dataset and refer the reader to Appendix A.13 for additional experiments on CIFAR-100 and SVHN, including comparisons with random and oracle *Top-k L2D* baselines. Implementation details and further discussion of the training setup are also provided in Appendix A.13. The evaluation metrics used are formally defined in Appendices A.12 and A.13.2. Algorithms for both *Top-k* and *Top-k(x) L2D* are provided in Appendix A.1, along with visual illustrations in Appendix A.2.

Figure 1: Performance of *Top-k* and *Top-k(x) L2D* across varying budget $\bar{\beta}$. Each plot reports a different metric: (a) minimum RMSE, (b) uniform average RMSE, and (c) weighted average RMSE.



In Figure 1a, *Top-k(x)* achieves near-optimal performance (6.23) with a budget of $\bar{\beta} = 0.156$ and an expected number of agents $\bar{k} = 4.77$, whereas *Top-k* requires the full budget $\bar{\beta} = 0.2$ and $\bar{k} = 6$ to reach a comparable score (6.21). This demonstrates the ability of *Top-k(x)* to allocate resources more efficiently by querying only the necessary number of agents, in contrast to *Top-k*, which tends to over-allocate costly or redundant experts. Additionally, our approach outperforms the Top-1 L2D baseline (Mao et al., 2024), confirming the limitations of single-agent deferral in regression tasks.

Figures 1b and 1c evaluate *Top-k* and *Top-k(x) L2D* under more restrictive metrics—RMSE_{avg} and RMSE_{w-avg}—where performance is not necessarily monotonic in the number of queried agents. In these settings, consulting too many or overly expensive agents may degrade overall performance. *Top-k(x)* consistently outperforms *Top-k* by carefully adjusting the number of consulted agents. In both cases, it achieves optimal performance with a budget of only $\bar{\beta} = 0.095$, a level that *Top-k* fails to reach. For example, in Figure 1b, *Top-k(x)* achieves RMSE_{avg} = 8.53, compared to 10.08 for *Top-k*. Similar trends are observed under the weighted average metric (Figure 1c), where *Top-k(x)* again outperforms *Top-k*, suggesting that incorporating rejector-derived weights w_j leads to more effective aggregation.

6 Conclusion

We introduced *Top-k Learning-to-Defer*, a generalization of the two-stage L2D framework that allows deferring queries to multiple agents, and its adaptive extension *Top-k(x) L2D*, which dynamically selects the number of consulted agents based on input complexity, consultation costs, and agents underlying distributions. We established rigorous theoretical guarantees, including Bayes and $(\mathcal{R}, \mathcal{G})$ -consistency, and showed that model cascades arise as a restricted special case of our framework.

Through extensive experiments on both classification and regression tasks, we demonstrated that *Top-k L2D* consistently outperforms single-agent deferral baselines. Moreover, *Top-k(x) L2D* further improves performance by achieving comparable or better accuracy at a lower consultation cost. These results highlight the importance of adaptive, cost-aware expert allocation in multi-agent decision systems.

References

- Awasthi, P., Mao, A., Mohri, M., and Zhong, Y. (2022). Multi-class h-consistency bounds. In *Proceedings of the 36th International Conference on Neural Information Processing Systems, NIPS '22*, Red Hook, NY, USA. Curran Associates Inc.
- Bartlett, P., Jordan, M., and McAuliffe, J. (2006). Convexity, classification, and risk bounds. *Journal of the American Statistical Association*, 101:138–156.
- Bartlett, P. L. and Wegkamp, M. H. (2008). Classification with a reject option using a hinge loss. *The Journal of Machine Learning Research*, 9:1823–1840.
- Chow, C. (1970). On optimum recognition error and reject tradeoff. *IEEE Transactions on Information Theory*, 16(1):41–46.
- Cortes, C., DeSalvo, G., and Mohri, M. (2016). Learning with rejection. In Ortner, R., Simon, H. U., and Zilles, S., editors, *Algorithmic Learning Theory*, pages 67–82, Cham. Springer International Publishing.
- Cortes, C., Mao, A., Mohri, C., Mohri, M., and Zhong, Y. (2024). Cardinality-aware set prediction and top- k classification. In *The Thirty-eighth Annual Conference on Neural Information Processing Systems*.
- Cortes, C. and Vapnik, V. N. (1995). Support-vector networks. *Machine Learning*, 20:273–297.
- Dietterich, T. G. (2000). Ensemble methods in machine learning. In *Multiple Classifier Systems*, pages 1–15, Berlin, Heidelberg. Springer Berlin Heidelberg.
- Dohan, D., Xu, W., Lewkowycz, A., Austin, J., Bieber, D., Lopes, R. G., Wu, Y., Michalewski, H., Saurous, R. A., Sohl-Dickstein, J., et al. (2022). Language model cascades. *arXiv preprint arXiv:2207.10342*.
- Fatima, M., Pasha, M., et al. (2017). Survey of machine learning algorithms for disease diagnostic. *Journal of Intelligent Learning Systems and Applications*, 9(01):1.
- Geifman, Y. and El-Yaniv, R. (2017). Selective classification for deep neural networks. In Guyon, I., Luxburg, U. V., Bengio, S., Wallach, H., Fergus, R., Vishwanathan, S., and Garnett, R., editors, *Advances in Neural Information Processing Systems*, volume 30. Curran Associates, Inc.
- Ghosh, A., Kumar, H., and Sastry, P. S. (2017). Robust loss functions under label noise for deep neural networks. In *Proceedings of the Thirty-First AAAI Conference on Artificial Intelligence, AAAI'17*, page 1919–1925. AAAI Press.
- Goodfellow, I. J., Bulatov, Y., Ibarz, J., Arnoud, S., and Shet, V. (2014). Multi-digit number recognition from street view imagery using deep convolutional neural networks.
- He, K., Zhang, X., Ren, S., and Sun, J. (2015). Deep residual learning for image recognition.
- Jiang, Y., Nishikawa, R. M., Schmidt, R. A., Metz, C. E., Giger, M. L., and Doi, K. (1999). Improving breast cancer diagnosis with computer-aided diagnosis. *Academic radiology*, 6(1):22–33.
- Jitkrittum, W., Gupta, N., Menon, A. K., Narasimhan, H., Rawat, A. S., and Kumar, S. (2024). When does confidence-based cascade deferral suffice?
- Kelley Pace, R. and Barry, R. (1997). Sparse spatial autoregressions. *Statistics and Probability Letters*, 33(3):291–297.
- Kingma, D. P. and Ba, J. (2017). Adam: A method for stochastic optimization.
- Krizhevsky, A. (2009). Learning multiple layers of features from tiny images.
- Lapin, M., Hein, M., and Schiele, B. (2015). Top-k multiclass svm.
- Lapin, M., Hein, M., and Schiele, B. (2016a). Analysis and optimization of loss functions for multiclass, top-k, and multilabel classification.

- Lapin, M., Hein, M., and Schiele, B. (2016b). Loss functions for top-k error: Analysis and insights.
- Laskaridis, S., Kouris, A., and Lane, N. D. (2021). Adaptive inference through early-exit networks: Design, challenges and directions. In *Proceedings of the 5th International Workshop on Embedded and Mobile Deep Learning, EMDL'21*, page 1–6, New York, NY, USA. Association for Computing Machinery.
- Loshchilov, I. and Hutter, F. (2019). Decoupled weight decay regularization.
- Madras, D., Pitassi, T., and Zemel, R. (2018). Predict responsibly: Improving fairness and accuracy by learning to defer.
- Mao, A., Mohri, C., Mohri, M., and Zhong, Y. (2023a). Two-stage learning to defer with multiple experts. In *Thirty-seventh Conference on Neural Information Processing Systems*.
- Mao, A., Mohri, M., and Zhong, Y. (2023b). Cross-entropy loss functions: Theoretical analysis and applications.
- Mao, A., Mohri, M., and Zhong, Y. (2024). Regression with multi-expert deferral.
- Mohri, M., Rostamizadeh, A., and Talwalkar, A. (2012). *Foundations of machine learning*. MIT Press.
- Montreuil, Y., Carlier, A., Ng, L. X., and Ooi, W. T. (2025a). Adversarial robustness in two-stage learning-to-defer: Algorithms and guarantees.
- Montreuil, Y., Yeo, S. H., Carlier, A., Ng, L. X., and Ooi, W. T. (2024). Two-stage learning-to-defer for multi-task learning.
- Montreuil, Y., Yeo, S. H., Carlier, A., Ng, L. X., and Ooi, W. T. (2025b). Optimal query allocation in extractive qa with llms: A learning-to-defer framework with theoretical guarantees.
- Mozannar, H., Lang, H., Wei, D., Sattigeri, P., Das, S., and Sontag, D. A. (2023). Who should predict? exact algorithms for learning to defer to humans. In *International Conference on Artificial Intelligence and Statistics*.
- Mozannar, H. and Sontag, D. (2020). Consistent estimators for learning to defer to an expert. In *Proceedings of the 37th International Conference on Machine Learning, ICML'20*. JMLR.org.
- Narasimhan, H., Jitkrittum, W., Menon, A. K., Rawat, A., and Kumar, S. (2022). Post-hoc estimators for learning to defer to an expert. In Koyejo, S., Mohamed, S., Agarwal, A., Belgrave, D., Cho, K., and Oh, A., editors, *Advances in Neural Information Processing Systems*, volume 35, pages 29292–29304. Curran Associates, Inc.
- Ohn Aldrich, R. A. (1997). Fisher and the making of maximum likelihood 1912-1922. *Statistical Science*, 12(3):162–179.
- Palomba, F., Pugnana, A., Alvarez, J. M., and Ruggieri, S. (2025). A causal framework for evaluating deferring systems. In *The 28th International Conference on Artificial Intelligence and Statistics*.
- Radford, A., Kim, J. W., Hallacy, C., Ramesh, A., Goh, G., Agarwal, S., Sastry, G., Askell, A., Mishkin, P., Clark, J., Krueger, G., and Sutskever, I. (2021). Learning transferable visual models from natural language supervision.
- Saberian, M. and Vasconcelos, N. (2014). Boosting algorithms for detector cascade learning. *Journal of Machine Learning Research*, 15(74):2569–2605.
- Steinwart, I. (2007). How to compare different loss functions and their risks. *Constructive Approximation*, 26:225–287.
- Strong, J., Men, Q., and Noble, A. (2024). Towards human-AI collaboration in healthcare: Guided deferral systems with large language models. In *ICML 2024 Workshop on LLMs and Cognition*.
- Tewari, A. and Bartlett, P. L. (2007). On the consistency of multiclass classification methods. *Journal of Machine Learning Research*, 8(36):1007–1025.

- Thilagar, A., Frongillo, R., Finocchiaro, J. J., and Goodwill, E. (2022). Consistent polyhedral surrogates for top-k classification and variants. In Chaudhuri, K., Jegelka, S., Song, L., Szepesvari, C., Niu, G., and Sabato, S., editors, *Proceedings of the 39th International Conference on Machine Learning*, volume 162 of *Proceedings of Machine Learning Research*, pages 21329–21359. PMLR.
- Verma, R., Barrejon, D., and Nalisnick, E. (2022). Learning to defer to multiple experts: Consistent surrogate losses, confidence calibration, and conformal ensembles. In *International Conference on Artificial Intelligence and Statistics*.
- Viola, P. and Jones, M. (2001). Rapid object detection using a boosted cascade of simple features. In *Proceedings of the 2001 IEEE Computer Society Conference on Computer Vision and Pattern Recognition. CVPR 2001*, volume 1, pages I–I.
- Wang, Y. and Scott, C. (2023). On classification-calibration of gamma-phi losses. In Neu, G. and Rosasco, L., editors, *Proceedings of Thirty Sixth Conference on Learning Theory*, volume 195 of *Proceedings of Machine Learning Research*, pages 4929–4951. PMLR.
- Weston, J. and Watkins, C. (1998). Multi-class support vector machines. Technical report, Citeseer.
- Yang, F. and Koyejo, S. (2020). On the consistency of top-k surrogate losses.
- Zhang, M. and Agarwal, S. (2020). Bayes consistency vs. h-consistency: The interplay between surrogate loss functions and the scoring function class. In Larochelle, H., Ranzato, M., Hadsell, R., Balcan, M., and Lin, H., editors, *Advances in Neural Information Processing Systems*, volume 33, pages 16927–16936. Curran Associates, Inc.
- Zhang, T. (2002). Statistical behavior and consistency of classification methods based on convex risk minimization. *Annals of Statistics*, 32.
- Zhang, Z. and Sabuncu, M. R. (2018). Generalized cross entropy loss for training deep neural networks with noisy labels.

Contents

1	Introduction	1
2	Related Work	2
3	Preliminaries	3
4	Top-k Learning-to-Defer	4
4.1	Introducing the Top- k Learning-to-Defer Problem	5
4.2	Top- k L2D: Introducing the Surrogate for the Top- k Deferral Loss	5
4.3	Theoretical Guarantees	6
4.3.1	Optimality of the Rejector Set	6
4.3.2	Consistency of Top- k Deferral Surrogates	7
4.4	Top- $k(x)$ L2D: Selecting the Optimal Number of Agents $k(x)$ Per Query	7
5	Experiments	9
6	Conclusion	9
	Appendix	13
A	Appendix	15
A.1	Algorithm	15
A.2	Illustration of Top- $k(x)$ and Top- k L2D	15
A.3	Notations	17
A.4	Model Cascades Are Special Cases of Top- k and Top- $k(x)$ L2D	17
A.4.1	Model cascades	17
A.4.2	Embedding a fixed- k cascade	18
A.4.3	Embedding adaptive (early-exit) cascades	18
A.5	Expressiveness: Model Cascades vs. Top- k / Top- $k(x)$ L2D	18
A.6	Proof Lemma 4.2	19
A.7	Proof Lemma 4.3	20
A.8	Proof Corollary 4.4	21
A.9	Proof Lemma 4.5	21
A.10	Proof Theorem 4.6	23
A.11	Proof Lemma 4.8	25
A.12	Choice of the metric d	26
A.13	Experiments	27
A.13.1	Datasets	27
A.13.2	Metrics	27
A.13.3	General Settings for Top- k and Top- $k(x)$ L2D	27
A.13.4	Reproducibility	28

A.14 Resources	28
A.14.1 Results on California Housing	28
A.14.2 Results on SVHN	29
A.14.3 Results on CIFAR100.	31

A Appendix

A.1 Algorithm

Algorithm 1 Top- k L2D Training Algorithm

Input: Dataset $\{(x_i, z_i)\}_{i=1}^I$, main model $g \in \mathcal{G}$, experts $m = (m_1, \dots, m_J)$, rejector $r \in \mathcal{R}$, number of epochs EPOCH, batch size BATCH, learning rate μ .

Initialization: Initialize rejector parameters θ .

for $i = 1$ to EPOCH **do**

Shuffle dataset $\{(x_i, z_i)\}_{i=1}^I$.

for each mini-batch $\mathcal{B} \subset \{(x_i, z_i)\}_{i=1}^I$ of size BATCH **do**

Extract input-output pairs $(x, z) \in \mathcal{B}$.

Query model $g(x)$ and experts $m(x)$. { Agents have been trained offline and fixed }

Evaluate aggregated costs $\tau_j(a(x), z)$ for $j \in \mathcal{A}$ agents. { Compute costs }

Compute the empirical risk minimization:

$$\hat{\mathcal{E}}_{\Phi_{\text{def},k}}(r; \theta) = \frac{1}{\text{BATCH}} \sum_{z \in \mathcal{B}} \left[\Phi_{\text{def},k}^u(r, a, x, z) \right].$$

Update parameters θ :

$$\theta \leftarrow \theta - \mu \nabla_{\theta} \hat{\mathcal{E}}_{\Phi_{\text{def},k}}(r; \theta). \quad \text{{ Gradient update }}$$

end for

end for

Return: trained rejector model \hat{r} .

Algorithm 2 Cardinality Training Algorithm

Input: Dataset $\{(x_i, z_i)\}_{i=1}^I$, main model $g \in \mathcal{G}$, experts $m = (m_1, \dots, m_J)$, trained rejector \hat{r} from Algorithm 1, selector $s \in \mathcal{S}$, number of epochs EPOCH, batch size BATCH, learning rate μ .

Initialization: Initialize selector parameters θ .

for $i = 1$ to EPOCH **do**

Shuffle dataset $\{(x_i, z_i)\}_{i=1}^I$.

for each mini-batch $\mathcal{B} \subset \{(x_i, z_i)\}_{i=1}^I$ of size BATCH **do**

Extract input-output pairs $(x, z) \in \mathcal{B}$.

Query model $g(x)$ and experts $m(x)$. { Agents have been trained offline and fixed }

Compute the scores $\{\hat{r}(x, j)\}_{j=0}^J$ using the trained rejector $\hat{r}(x)$.

Sort these scores and select entries to construct the rejector set $\hat{R}_{|\mathcal{A}|}(x)$.

Compute the empirical risk minimization:

$$\hat{\mathcal{E}}_{\Phi_{\text{car}}}(s; \theta) = \frac{1}{\text{BATCH}} \sum_{z \in \mathcal{B}} \left[\Phi_{\text{car}}(\hat{R}_{|\mathcal{A}|}, s, a(x), z) \right].$$

Update parameters θ :

$$\theta \leftarrow \theta - \mu \nabla_{\theta} \hat{\mathcal{E}}_{\Phi_{\text{car}}}(s; \theta). \quad \text{{ Gradient update }}$$

end for

end for

Return: trained selector model \hat{s} .

A.2 Illustration of Top- $k(x)$ and Top- k L2D

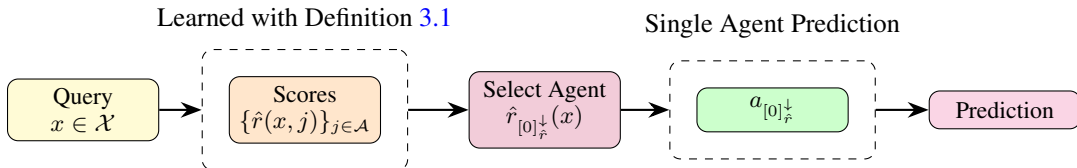


Figure 2: Inference step of Top-1 L2D (Narasimhan et al., 2022; Mao et al., 2023a, 2024; Montreuil et al., 2024): Given a query, we process it through the rejector. We select the agent with the highest score $r(x) = \arg \max_{j \in \mathcal{A}} r(x, j)$. Then, we query this agent and make the final prediction.

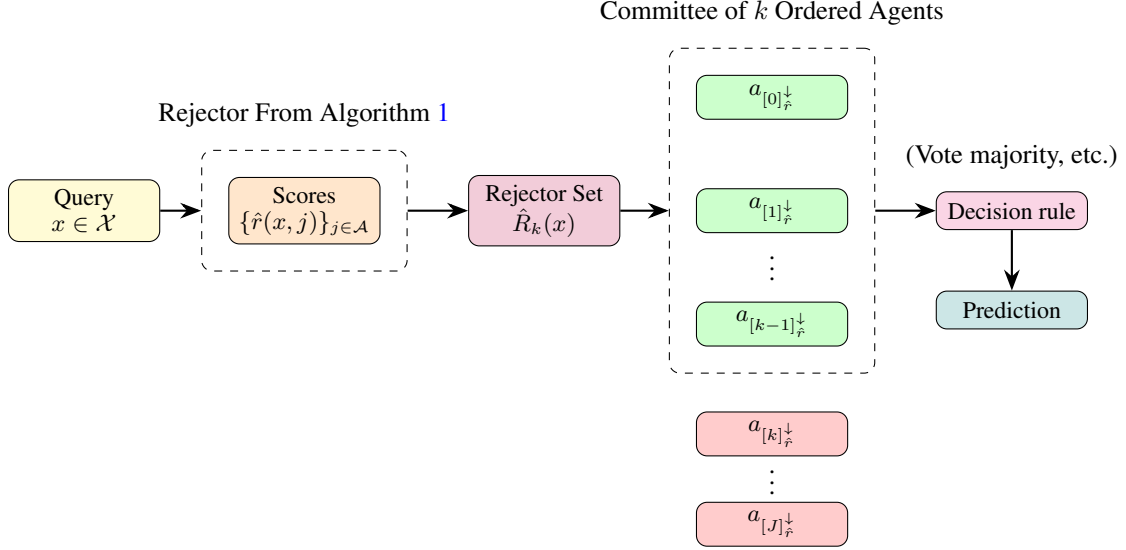


Figure 3: Inference Step of Top- k L2D: Given a query x , we first process it through the rejctor trained using Algorithm 1. Based on this, we select a fixed number k of agents to query, forming the *Rejctor Set* $R_k(x)$, as defined in Definition 4.1. By construction, the expected size satisfies $\mathbb{E}_x[|R_k(x)|] = k$. We then aggregate predictions from the selected top- k agents using a decision rule—such as majority vote or weighted voting. The final prediction is produced by this committee according to the chosen rule.

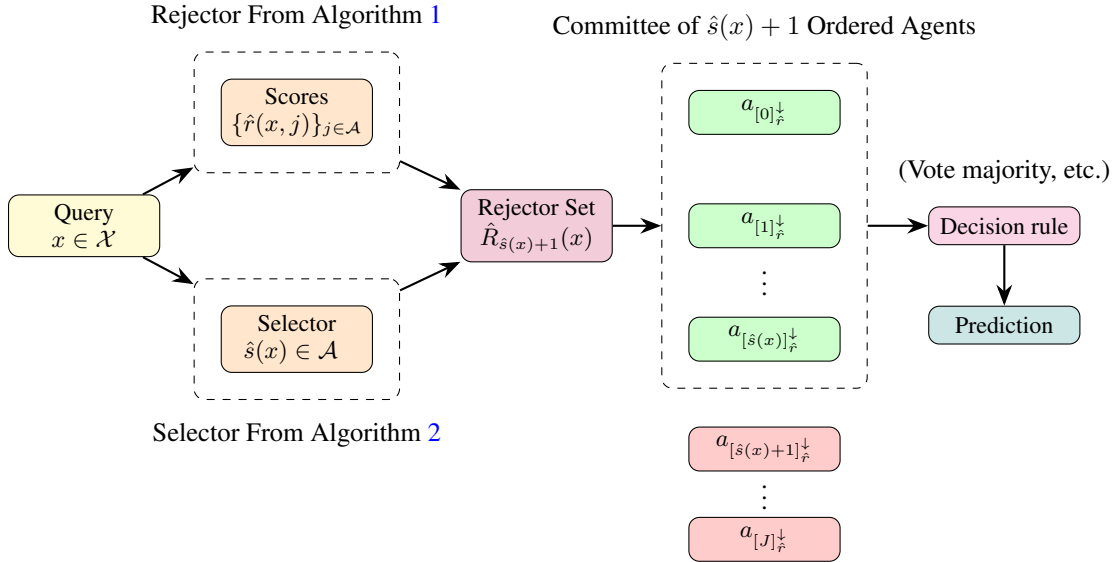


Figure 4: Inference Step of Top- $k(x)$ L2D: Given a query x , we process it through both the rejctor, trained using Algorithm 1, and the selector, trained using Algorithm 2. Based on these two functions, we construct the *Rejctor Set*, as defined in Definition 4.1. By construction, its expected size satisfies $\mathbb{E}_x[|\hat{R}_{\hat{s}(x)+1}(x)|] = \mathbb{E}_x[k(x)]$. We then aggregate predictions from the top- $(\hat{s}(x) + 1)$ agents using a decision rule (e.g., majority vote, weighted voting). The final prediction is produced by this committee of experts according to the chosen decision rule.

In the subsequent subsection, we will prove key lemmas, corollary and theorem from the main paper.

A.3 Notations

Definition A.1 (Orderings on a finite set). Let $\Omega = \{1, \dots, N\}$ be a set of cardinality $N := |\Omega|$ and let

$$f : \mathcal{M} \times \Omega \longrightarrow \mathbb{R}, \quad (m, \omega) \mapsto f(m, \omega),$$

where \mathcal{M} is a measurable input space (typically $\mathcal{M} = \mathcal{X}$ or $\mathcal{M} = \mathcal{X} \times \mathcal{Y}$).

Descending permutation. For every fixed $m \in \mathcal{M}$, let

$$\pi_f^\downarrow(m) : \Omega \longrightarrow \Omega$$

be the (tie-broken) permutation that satisfies

$$f(m, \pi_f^\downarrow(m)(1)) \geq f(m, \pi_f^\downarrow(m)(2)) \geq \dots \geq f(m, \pi_f^\downarrow(m)(N)).$$

The element occupying the i -th *largest* position is denoted by

$$[i]_f^\downarrow := \pi_f^\downarrow(m)(i), \quad i = 1, \dots, N.$$

Ascending permutation. Analogously, define

$$\pi_f^\uparrow(m) : \Omega \longrightarrow \Omega$$

such that

$$f(m, \pi_f^\uparrow(m)(1)) \leq f(m, \pi_f^\uparrow(m)(2)) \leq \dots \leq f(m, \pi_f^\uparrow(m)(N)),$$

and set

$$[i]_f^\uparrow := \pi_f^\uparrow(m)(i), \quad i = 1, \dots, N.$$

Top- k subset. For $k \in \{0, \dots, J\}$ and an order indicator $o \in \{\downarrow, \uparrow\}$, the *top- k subset* is

$$R_k(x) := \{[0]_f^o, [1]_f^o, \dots, [k-1]_f^o\}.$$

Remark 6 (Typical instantiations). In particular:

1. **Rejector scores.** Take $\Omega = \mathcal{A} = \{0, \dots, J\}$, $\mathcal{M} = \mathcal{X}$, and $f_r(x, j) := r(x, j)$. Descending order ($o = \downarrow$) ranks agents from most to least confident at retaining the query.
2. **Agent-specific consultation costs.** Fix $\Omega = \mathcal{A}$ but enlarge the input space to $\mathcal{M} = \mathcal{X} \times \mathcal{Z}$ and define

$$f_c((x, z), j) := c_j(a_j(x), z).$$
 Ascending order ($o = \uparrow$) lists agents from cheapest to most expensive for the specific pair (x, z) .
3. **Label-wise scores.** Let $\Omega = \mathcal{Y}$ (label set), $\mathcal{M} = \mathcal{X}$, and $f_h(x, y) := h(x, y)$. Either order can be used, depending on whether larger or smaller h -values are preferable for prediction.

A.4 Model Cascades Are Special Cases of Top- k and Top- $k(x)$ L2D

Throughout, let $\mathcal{A} = \{0\} \cup [J]$ be the index set of agents, already introduced in Section 3. For $j \in \mathcal{A}$ we denote by $a_j : \mathcal{X} \rightarrow \mathcal{Z}$ the prediction of agent j , by $r : \mathcal{X} \times \mathcal{A} \rightarrow \mathbb{R}$ a *rejector score*, and by $R_k(x) = \{r_{[0]_r^\downarrow}(x), \dots, r_{[k-1]_r^\downarrow}(x)\}$ the *rejector set* containing the indices of the k largest scores (Definition 4.1).

A.4.1 Model cascades

Definition A.2 (Evaluation order and thresholds). Fix a permutation $\rho = (\rho_0, \rho_1, \dots, \rho_J)$ of \mathcal{A} (the *evaluation order*) and confidence thresholds $0 < \mu_0 < \mu_1 < \dots < \mu_J < 1$. For each agent let $\text{conf} : \mathcal{X} \times \mathcal{A} \rightarrow [0, 1]$ be a confidence measure.

Definition A.3 (Size- k cascade allocation). For a fixed $k \in \{1, \dots, |\mathcal{A}|\}$ define the *cascade set*

$$\mathcal{K}_k(x) := \{\rho_0, \rho_1, \dots, \rho_{k-1}\}.$$

The cascade evaluates the agents in the order ρ until it reaches ρ_{k-1} . If the confidence test $\text{conf}(\rho_{k-1}, x) \geq \mu_{k-1}$ is satisfied, the cascade *allocates* the set $\mathcal{K}_k(x)$; otherwise it proceeds to the next stage (see Section A.4.3 for the adaptive case).

A.4.2 Embedding a fixed- k cascade

Lemma A.4 (Score construction). *For a fixed k define*

$$r_k(x, j) := \begin{cases} 2 - \frac{\text{rank}_{\mathcal{K}_k(x)}(j)}{k+1}, & j \in \mathcal{K}_k(x), \\ -\frac{\text{rank}_{\mathcal{A} \setminus \mathcal{K}_k(x)}(j)}{J+1}, & j \notin \mathcal{K}_k(x), \end{cases}$$

where $\text{rank}_B(j) \in \{1, \dots, |B|\}$ is the index of j inside the list B ordered according to ρ . Then for every $x \in \mathcal{X}$

$$R_k(x) = \mathcal{K}_k(x).$$

Proof. Separation. Scores assigned to $\mathcal{K}_k(x)$ lie in $(1, 2]$, while scores assigned to $\mathcal{A} \setminus \mathcal{K}_k(x)$ lie in $[-1, -\frac{1}{J+1}]$; hence all k largest scores belong exactly to $\mathcal{K}_k(x)$.

Distinctness. Within each block, consecutive ranks differ by $1/(k+1)$ or $1/(J+1)$, so ties cannot occur. Therefore the permutation returns precisely the indices of $\mathcal{K}_k(x)$ in decreasing order, and the rejector set equals $\mathcal{K}_k(x)$. \square

Corollary A.5 (Cascade embedding for any fixed k). *For every $k \in \{1, \dots, |\mathcal{A}|\}$ the rejector r_k of Lemma A.4 satisfies*

$$R_k(x) = \mathcal{K}_k(x) \quad \forall x \in \mathcal{X}.$$

Consequently, the Top- k Learning-to-Defer allocation coincides exactly with the size- k cascade allocation.

Proof. Immediate from Lemma A.4. \square

A.4.3 Embedding adaptive (early-exit) cascades

Let the cascade stop after a *data-dependent* number of stages $k(x) \in \{1, \dots, |\mathcal{A}|\}$. Define the selector $s(x) = k(x) + 1$ (as required in Section 4.4) and reuse the score construction of Lemma A.4 with k replaced by $k(x)$: $r_{k(x)}(x, \cdot)$.

Lemma A.6 (Cascade embedding for adaptive cardinality). *With rejector $r_{k(x)}$ and selector $s(x) = k(x) + 1$ the Top- $k(x)$ Learning-to-Defer pipeline allocates $\mathcal{K}_{k(x)}(x)$ for every input x . Therefore any adaptive (early-exit) model cascade is a special case of Top- $k(x)$ Learning-to-Defer.*

Proof. Applying Lemma A.4 with $k = k(x)$ yields $R_{k(x)}(x) = \mathcal{K}_{k(x)}(x)$. The selector truncates the full rejector set to its first $s(x) + 1 = k(x)$ elements—precisely $\mathcal{K}_{k(x)}(x)$. \square

Remark (Theoretical guarantees). Since the rejectors constructed above belong to the complete, regular and symmetric hypothesis class \mathcal{R} assumed in Theorem 4.6, all surrogate-risk guarantees (Bayes and $(\mathcal{G}, \mathcal{R})$ -consistency) established for Top- k and Top- $k(x)$ Learning-to-Defer *automatically extend* to classical model cascades.

A.5 Expressiveness: Model Cascades vs. Top- k / Top- $k(x)$ L2D

Hierarchy. Every model cascade can be realised by a suitable choice of rejector scores and, for the adaptive case, a selector (see App. A.4). Hence

$$\underbrace{\text{Model Cascades}}_{\text{prefix of a fixed order}} \subset \underbrace{\text{Top-}k \text{ L2D}}_{\text{constant } k} \subset \underbrace{\text{Top-}k(x) \text{ L2D}}_{\text{learned } k(x)}.$$

The inclusion is *strict*, for the reasons detailed below.

Why the inclusion is strict.

1. **Non-contiguous selection.** A Top- k rejector may pick any subset of size k (e.g. $\{0, 2, 5\}$), whereas a cascade always selects a *prefix* $\{\rho_0, \dots, \rho_{k-1}\}$ of the evaluation order.
2. **Learned cardinality.** In Top- $k(x)$ L2D the selector $s(x)$ is trained by minimising the cardinality surrogate; Theorem 4.6 provides $(\mathcal{G}, \mathcal{R})$ -consistency. Classical cascades rely on fixed confidence thresholds with no statistical guarantee.
3. **Cost-aware ordering.** Lemma 4.5 shows the Bayes-optimal rejector orders agents by *expected cost*, which may vary with x . Cascades usually impose a single, input-independent order ρ .
4. **Multi-expert aggregation.** After selecting k agents, Top- k L2D can aggregate their predictions (majority vote, weighted vote, averaging, *etc.*). A cascade stops at the *first* confident agent and discards all later opinions.

Separating example. Consider three models a_0, a_1, a_2 . A Top-2 policy that always chooses the two most confident models (e.g. $\{0, 2\}$ on some inputs, $\{1, 2\}$ on others) and combines them by weighted voting *cannot* be written as a cascade: no prefix of a fixed order can realise the non-contiguous set $\{0, 2\}$, and cascades output a single agent rather than a pair. Therefore Top- k /Top- $k(x)$ Learning-to-Defer is strictly more expressive than classical model cascades.

A.6 Proof Lemma 4.2

Lemma 4.2 (Top- k Deferral Loss). *Let $x \in \mathcal{X}$ be a query and $R_k(x) \subseteq \mathcal{A}$ the rejector set from Definition 4.1. The top- k deferral loss is defined as:*

$$\ell_{\text{def},k}(R_k(x), a(x), x, z) = \sum_{j=0}^J c_j(a_j(x), z) \mathbf{1}_{j \in R_k(x)}.$$

Proof. In the standard L2D setting (see 3.1), the deferral loss utilizes the indicator function $\mathbf{1}_{r(x)=j}$ to select the most cost-efficient agent in the system. We can upper-bound the standard L2D loss by employing the indicator function over the rejector set $R_k(x)$:

$$\begin{aligned} \ell_{\text{def}}(r(x), a, x, z) &= \sum_{j=0}^J c_j(a_j(x), z) \mathbf{1}_{r(x)=j} \\ &\leq \sum_{j=0}^J c_j(a_j(x), z) \mathbf{1}_{j \in R_k(x)} \\ &= \ell_{\text{def},k}(R_k(x), a(x), x, z). \end{aligned} \tag{4}$$

Consider a system with three agents, $\mathcal{A} = \{0, 1, 2\}$, and a rejector set $R_{k=|\mathcal{A}|}(x) = \{2, 1, 0\}$. This indicates that agent 2 has a higher confidence score than agent 1 and 0, i.e., $r(x, 2) \geq r(x, 1) \geq r(x, 0)$. We evaluate $\ell_{\text{def},k}$ for different values of $k \leq |\mathcal{A}|$:

For $k = 1$: The rejector set is $R_1(x) = \{2\}$, which corresponds to the standard L2D setting where deferral is made to the most confident agent (Narasimhan et al., 2022; Mao et al., 2023a). Thus,

$$\ell_{\text{def},1}(R_1(x), a, x, z) = c_2(a_2(x), z), \tag{5}$$

recovering the same result as ℓ_{def} .

For $k = 2$: The rejector set expands to $R_2(x) = \{2, 1\}$, implying that both agent 2 and agent 1 are queried. Therefore,

$$\ell_{\text{def},2}(R_2(x), a, x, z) = c_2(a_2(x), z) + c_1(a_1(x), z), \tag{6}$$

correctly reflecting the computation of costs from the queried agents.

For $k = 3$: The rejector set further extends to $R_3(x) = \{2, 1, 0\}$, implying that all agents in the system are queried. Consequently,

$$\ell_{\text{def},3}(R_3(x), a, x, z) = c_2(a_2(x), z) + c_1(a_1(x), z) + c_0(a_0(x), z), \tag{7}$$

incorporating the costs from all agents in the system. \square

A.7 Proof Lemma 4.3

Lemma 4.3 (Upper-Bounding the Top- k Deferral Loss). *Let $x \in \mathcal{X}$ be an input, and $k \leq |\mathcal{A}|$ the size of the rejector set. Then, the top- k deferral loss satisfies:*

$$\ell_{\text{def},k}(R_k(x), a(x), x, z) \leq \sum_{j=0}^J \tau_j(a(x), z) \Phi_{01}^u(r, x, j) - (J - k) \sum_{j=0}^J c_j(a_j(x), z).$$

Proof. We establish an upper bound on the top- k deferral loss, which involves the multi-class classification loss Φ_{01}^u . First, we recall the definition of the top- k deferral loss:

$$\ell_{\text{def},k}(R_k(x), a(x), x, z) = \sum_{j=0}^J c_j(a_j(x), z) \mathbf{1}_{j \in R_k(x)}. \quad (8)$$

To facilitate the derivation of a surrogate top- k loss, we explicitly express the top- k deferral loss in terms of the top- k classification loss ℓ_k , utilizing the fact that $\Phi_{01}^u \geq \ell_k$ (Lapin et al., 2015; Cortes et al., 2024).

Given the rejector set $R_k(x) = \{r_{[0]_r^\downarrow}(x), \dots, r_{[k-1]_r^\downarrow}(x)\}$, we express the indicator function as

$$\mathbf{1}_{j \in R_k(x)} = \sum_{i=0}^{k-1} \mathbf{1}_{r_{[i]_r^\downarrow}(x)=j}, \quad (9)$$

where we use the fact that the elements of $R_k(x)$ are distinct. We further decompose this expression:

$$\mathbf{1}_{j \in R_k(x)} = \sum_{i=0}^{k-1} \left(\sum_{q=0}^J \mathbf{1}_{r_{[i]_r^\downarrow}(x) \neq q} \mathbf{1}_{q \neq j} - (J - 1) \right). \quad (10)$$

Rearranging, we obtain

$$\mathbf{1}_{j \in R_k(x)} = \sum_{i=0}^{k-1} \sum_{q=0}^J \mathbf{1}_{r_{[i]_r^\downarrow}(x) \neq q} \mathbf{1}_{q \neq j} - k(J - 1). \quad (11)$$

Substituting this into the loss expression, we derive

$$\begin{aligned} \ell_{\text{def},k}(R_k(x), a(x), x, z) &= \sum_{j=0}^J c_j(a_j(x), z) \left(\sum_{i=0}^{k-1} \sum_{q=0}^J \mathbf{1}_{r_{[i]_r^\downarrow}(x) \neq q} \mathbf{1}_{q \neq j} - k(J - 1) \right) \\ &= \sum_{q=0}^J \sum_{i=0}^{k-1} \left(\sum_{j=0}^J c_j(a_j(x), z) \mathbf{1}_{q \neq j} \right) \mathbf{1}_{r_{[i]_r^\downarrow}(x) \neq q} - k(J - 1) \sum_{j=0}^J c_j(a_j(x), z). \end{aligned} \quad (12)$$

Defining $\tau_q(a(x), z) := \sum_{j=0}^J c_j(a_j(x), z) \mathbf{1}_{q \neq j}$, we rewrite the loss as

$$\ell_{\text{def},k}(R_k(x), a(x), x, z) = \sum_{q=0}^J \sum_{i=0}^{k-1} \tau_q(a(x), z) \mathbf{1}_{r_{[i]_r^\downarrow}(x) \neq q} - k(J - 1) \sum_{j=0}^J c_j(a_j(x), z). \quad (13)$$

Further simplification yields

$$\ell_{\text{def},k}(R_k(x), a(x), x, z) = \sum_{j=0}^J \tau_j(a(x), z) \sum_{i=0}^{k-1} \mathbf{1}_{r_{[i]_r^\downarrow}(x) \neq j} - k(J - 1) \sum_{j=0}^J c_j(a_j(x), z). \quad (14)$$

We now establish the expression for the sum $\sum_{i=0}^{k-1} \mathbf{1}_{r_{[i]_r^\downarrow}(x) \neq j}$. Given that each $r_{[i]_r^\downarrow}(x)$ is unique, we derive

$$\sum_{i=0}^{k-1} \mathbf{1}_{r_{[i]_r^\downarrow}(x) \neq j} = (k - 1) \mathbf{1}_{j \in R_k(x)} + k \mathbf{1}_{j \notin R_k(x)}. \quad (15)$$

This leads to

$$\begin{aligned}
\ell_{\text{def},k}(R_k(x), a(x), x, z) &= \sum_{j=0}^J \tau_j(a(x), z) \left((k-1) + 1_{j \notin R_k(x)} \right) - k(J-1) \sum_{j=0}^J c_j(a_j(x), z) \\
&= \sum_{j=0}^J \tau_j(a(x), z) 1_{j \notin R_k(x)} + (k-1)J \sum_{j=0}^J c_j(a_j(x), z) - k(J-1) \sum_{j=0}^J c_j(a_j(x), z) \\
&= \sum_{j=0}^J \tau_j(a(x), z) 1_{j \notin R_k(x)} - (J-k) \sum_{j=0}^J c_j(a_j(x), z) \\
&= \sum_{j=0}^J \tau_j(a(x), z) \ell_k(R_k(x), j) - (J-k) \sum_{j=0}^J c_j(a_j(x), z)
\end{aligned} \tag{16}$$

This loss exactly coincides with the usual L2D loss (Narasimhan et al., 2022; Mao et al., 2023a, 2024; Montreuil et al., 2024) by setting $k = 1$. Finally, using the fact that $\Phi_{01}^u \geq \ell_k$, we obtain the upper bound

$$\ell_{\text{def},k}(R_k(x), a(x), x, z) \leq \sum_{j=0}^J \tau_j(a(x), z) \Phi_{01}^u(r, x, j) - (J-k) \sum_{j=0}^J c_j(a_j(x), z). \tag{17}$$

We have proven an upper bound on $\ell_{\text{def},k}$. \square

A.8 Proof Corollary 4.4

Corollary 4.4 (Surrogate for the Top- k Deferral Loss). *Let $x \in \mathcal{X}$ be an input. The surrogate for the top- k deferral loss is defined as*

$$\Phi_{\text{def},k}^u(r, a, x, z) = \sum_{j=0}^J \tau_j(a(x), z) \Phi_{01}^u(r, x, j),$$

whose minimization is notably independent of the cardinality parameter k .

Proof. We begin with the previously established upper bound:

$$\ell_{\text{def},k}(R_k(x), a(x), x, z) \leq \sum_{j=0}^J \tau_j(a(x), z) \Phi_{01}^u(r, x, j) - (J-k) \sum_{j=0}^J c_j(a_j(x), z). \tag{18}$$

Since J and k are fixed parameters, the final surrogate loss does not necessarily need to retain the last term, as it does not affect the optimization over r . Dropping this term, we define the surrogate for the top- k deferral loss as:

$$\Phi_{\text{def},k}(r, a, x, z) = \sum_{j=0}^J \tau_j(a(x), z) \Phi_{01}^u(r, x, j). \tag{19}$$

This completes the proof. \square

A.9 Proof Lemma 4.5

Lemma 4.5 (Bayes-optimal Rejector Set). *For a given query $x \in \mathcal{X}$, the Bayes-optimal rejector set $R_k^B(x)$ is defined as the subset of k agents with the lowest expected costs, ordered in increasing cost:*

$$R_k^B(x) = \arg \min_{\substack{R_k(x) \subseteq \mathcal{A} \\ |R_k(x)|=k}} \sum_{j \in R_k(x)} \bar{c}_j^*(a_j(x), z) = \{[0]_{\bar{c}^*}^\dagger, [1]_{\bar{c}^*}^\dagger, \dots, [k-1]_{\bar{c}^*}^\dagger\},$$

where the ordering within $R_k^B(x)$ satisfies:

$$\forall j, j' \in R_k^B(x), \quad j < j' \implies \bar{c}_j^*(a_j(x), z) \leq \bar{c}_{j'}^*(a_{j'}(x), z).$$

Proof. To simplify notation, define the expected costs and the optimal expected costs

$$\bar{v}(g(x), z) = \mathbb{E}_{z|x}[v(g(x), z)] \quad \text{and} \quad v^*(g(x), z) = \inf_{g \in \mathcal{G}} v(g(x), z). \quad (20)$$

Let $R_k(x) \subseteq \mathcal{A}$ be a set of k agents. The conditional risk of the top- k deferral loss is then

$$\mathcal{C}_{\ell_{\text{def}}, k}(r, g, x) = \mathbb{E}_{z|x}[\ell_{\text{def}, k}(R_k(x), a(x), x, z)] = \sum_{j=0}^J \bar{c}_j(a_j(x), z) 1_{j \in R_k(x)}, \quad (21)$$

where each \bar{c}_j is the expectation (over $z \mid x$) of c_j . In classification, we would have $y \mid x$, in regression $t \mid x$.

The *Bayes-optimal* conditional risk is

$$\mathcal{C}_{\ell_{\text{def}}, k}^B(\mathcal{R}, \mathcal{G}, x) = \inf_{g \in \mathcal{G}, r \in \mathcal{R}} \mathcal{C}_{\ell_{\text{def}}, k}(r, g, x) = \inf_{r \in \mathcal{R}} \sum_{j=0}^J \bar{c}_j^*(a_j(x), z) 1_{j \in R_k(x)}, \quad (22)$$

where \bar{c}_j^* denotes the optimal expected cost for agent j . Minimizing this sum by choosing exactly k terms is equivalent to picking the k smallest values among $\{\bar{c}_j^* : 0 \leq j \leq J\}$. Sorting them in ascending order,

$$\bar{c}_{[0]_{\bar{c}^*}}^*(x) \leq \bar{c}_{[1]_{\bar{c}^*}}^*(x) \leq \dots \leq \bar{c}_{[J]_{\bar{c}^*}}^*(x), \quad (23)$$

the Bayes-optimal conditional risk becomes

$$\mathcal{C}_{\ell_{\text{def}}, k}^B(\mathcal{R}, \mathcal{G}, x) = \sum_{i=0}^{k-1} \bar{c}_{[i]_{\bar{c}^*}}^*(a_{[i]_{\bar{c}^*}}(x), z). \quad (24)$$

Consequently, the rejector set $R_k^B(x)$ that achieves this minimum is

$$R_k^B(x) = \arg \min_{\substack{R_k(x) \subseteq \mathcal{A} \\ |R_k(x)|=k}} \sum_{j \in R_k(x)} \bar{c}_j^*(a_j(x), z) = \{[0]_{\bar{c}^*}^\uparrow, [1]_{\bar{c}^*}^\uparrow, \dots, [k-1]_{\bar{c}^*}^\uparrow\}, \quad (25)$$

meaning $R_k^B(x)$ selects the k agents with the lowest optimal expected costs.

We have proven the desired result. \square

Remark 7. In the special case $k = 1$, this choice reduces to

$$\mathcal{C}_{\ell_{\text{def}}, 1}^B(\mathcal{R}, \mathcal{G}, x) = \min_{j \in \mathcal{A}} \bar{c}_j^*(a_j(x), z) = \bar{c}_{[0]_{\bar{c}^*}}^*(a_{[0]_{\bar{c}^*}}(x), z), \quad (26)$$

matching the usual L2D Bayes-conditional risk from (Mao et al., 2023a, 2024; Montreuil et al., 2024).

For instance, suppose the expected costs are:

$$\bar{c}_0^*(g(x), z) = 4, \quad \bar{c}_1(m_1(x), z) = 2, \quad \bar{c}_2(m_2(x), z) = 1. \quad (27)$$

Here, agent 2 has the lowest expected cost, followed by agent 1, and then agent 0. Applying the Bayes-optimal selection:

For $k = 1$:

$$R_1^B(x) = \{2\}, \quad (28)$$

since agent 2 has the lowest cost.

For $k = 2$:

$$R_2^B(x) = \{2, 1\}, \quad (29)$$

as agents 2 and 1 are the two most cost-efficient choices.

For $k = 3$:

$$R_3^B(x) = \{2, 1, 0\}. \quad (30)$$

In this case, the rejector set is ordered as $\{2, 1, 0\}$, meaning that the system selects the most cost-efficient agents in decreasing order of efficiency.

A.10 Proof Theorem 4.6

First, we prove an intermediate Lemma.

Lemma A.7 (Consistency of a Top- k Loss). *A surrogate loss function Φ_{01}^u is said to be \mathcal{R} -consistent with respect to the top- k loss ℓ_k if, for any $r \in \mathcal{R}$, there exists a concave, increasing, and non-negative function $\Gamma^u : \mathbb{R}^+ \rightarrow \mathbb{R}^+$ such that:*

$$\sum_{j \in \mathcal{A}} p_j 1_{j \notin R_k(x)} - \inf_{r \in \mathcal{R}} \sum_{j \in \mathcal{A}} p_j 1_{j \notin R_k(x)} \leq \Gamma^u \left(\sum_{j \in \mathcal{A}} p_j \Phi_{01}^u(r, x, j) - \inf_{r \in \mathcal{R}} \sum_{j \in \mathcal{A}} p_j \Phi_{01}^u(r, x, j) \right), \quad (31)$$

where $p \in \Delta^{|\mathcal{A}|}$ denotes a probability distribution over the set \mathcal{A} .

Proof. Assuming the following inequality holds:

$$\sum_{j \in \mathcal{A}} p_j 1_{j \notin R_k(x)} - \inf_{r \in \mathcal{R}} \sum_{j \in \mathcal{A}} p_j 1_{j \notin R_k(x)} \leq \Gamma^u \left(\sum_{j \in \mathcal{A}} p_j \Phi_{01}^u(r, x, j) - \inf_{r \in \mathcal{R}} \sum_{j \in \mathcal{A}} p_j \Phi_{01}^u(r, x, j) \right), \quad (32)$$

we identify the corresponding conditional risks for a distribution $p \in \Delta^{|\mathcal{A}|}$ as introduced by [Awasthi et al. \(2022\)](#):

$$\mathcal{C}_{\ell_k}(r, x) - \inf_{r \in \mathcal{R}} \mathcal{C}_{\ell_k}(r, x) \leq \Gamma^u \left(\mathcal{C}_{\Phi_{01}^u}(r, x) - \inf_{r \in \mathcal{G}} \mathcal{C}_{\Phi_{01}^u}(r, x) \right). \quad (33)$$

Using the definition from [Awasthi et al. \(2022\)](#), we express the expected conditional risk difference as:

$$\begin{aligned} \mathbb{E}_x[\Delta \mathcal{C}_{\ell_k}(r, x)] &= \mathbb{E}_x \left[\mathcal{C}_{\ell_k}(r, x) - \inf_{r \in \mathcal{R}} \mathcal{C}_{\ell_k}(r, x) \right] \\ &= \mathcal{E}_{\ell_k}(r) - \mathcal{E}_{\ell_k}^B(\mathcal{R}) - \mathcal{U}_{\ell_k}(\mathcal{R}). \end{aligned} \quad (34)$$

Consequently, we obtain:

$$\begin{aligned} \mathcal{C}_{\ell_k}(r, x) - \inf_{r \in \mathcal{R}} \mathcal{C}_{\ell_k}(r, x) &\leq \Gamma^u \left(\mathcal{C}_{\Phi_{01}^u}(r, x) - \inf_{r \in \mathcal{G}} \mathcal{C}_{\Phi_{01}^u}(r, x) \right), \\ \mathbb{E}_x[\Delta \mathcal{C}_{\ell_k}(r, x)] &\leq \Gamma^u \left(\mathbb{E}_x \left[\mathcal{C}_{\Phi_{01}^u}(r, x) \right] \right). \end{aligned} \quad (35)$$

By the concavity of Γ^u , applying Jensen's inequality yields:

$$\mathcal{E}_{\ell_k}(r) - \mathcal{E}_{\ell_k}^B(\mathcal{R}) - \mathcal{U}_{\ell_k}(\mathcal{R}) \leq \Gamma^u \left(\mathcal{E}_{\Phi_{01}^u}(r) - \mathcal{E}_{\Phi_{01}^u}^*(\mathcal{R}) - \mathcal{U}_{\Phi_{01}^u}(\mathcal{R}) \right). \quad (36)$$

This result implies that the surrogate loss Φ_{01}^u is \mathcal{R} -consistent with respect to the top- k loss ℓ_k , completing the proof. \square

Theorem 4.6 ($(\mathcal{G}, \mathcal{R})$ -Consistency Bound). *Let $x \in \mathcal{X}$, and consider a hypothesis class \mathcal{R} that is regular, complete, and symmetric, along with any distribution \mathcal{D} . Suppose the comp-sum surrogate family is \mathcal{R} -consistent. Then, there exists a non-decreasing, non-negative, concave function $\Gamma^u : \mathbb{R}^+ \rightarrow \mathbb{R}^+$, associated with the top- k loss ℓ_k and any surrogate from the comp-sum family parameterized with u , such that the following bound holds:*

$$\begin{aligned} \mathcal{E}_{\ell_{def,k}}(g, r) - \mathcal{E}_{\ell_{def,k}}^B(\mathcal{G}, \mathcal{R}) - \mathcal{U}_{\ell_{def,k}}(\mathcal{G}, \mathcal{R}) &\leq \tilde{\Gamma}^u \left(\mathcal{E}_{\Phi_{def,k}^u}(r) - \mathcal{E}_{\Phi_{def,k}^u}^*(\mathcal{R}) - \mathcal{U}_{\Phi_{def,k}^u}(\mathcal{R}) \right) \\ &\quad + \mathbb{E}_x \left[\bar{c}_0(g(x), z) - \inf_{g \in \mathcal{G}} \bar{c}_0(g(x), z) \right], \end{aligned}$$

where $\bar{c}_0(g(x), z) = \mathbb{E}_{z|x}[c_0(g(x), z)]$, $Q = \sum_{j=0}^J \mathbb{E}_{z|x}[\tau_j(a(x), z)]$, and $\tilde{\Gamma}^u(v) = Q \Gamma^u \left(\frac{v}{Q} \right)$.

Proof. We establish the consistency of the proposed top- k deferral surrogate by leveraging the results from Lemma 4.5 and its proof in A.9.

The conditional risk associated with the top- k deferral loss is given by:

$$\mathcal{C}_{\ell_{\text{def},k}}(r, g, x) = \sum_{j=0}^J \bar{c}_j(a_j(x), z) 1_{j \in R_k(x)}, \quad (37)$$

and the Bayes-optimal conditional risk is expressed as:

$$\mathcal{C}_{\ell_{\text{def},k}}^B(\mathcal{R}, \mathcal{G}, x) = \sum_{i=0}^{k-1} \bar{c}_{[i]_{\bar{c}^*}}^*(a_{[i]_{\bar{c}^*}}(x), z). \quad (38)$$

The calibration gap is then given by:

$$\begin{aligned} \Delta \mathcal{C}_{\ell_{\text{def},k}}(r, x) &= \mathcal{C}_{\ell_{\text{def},k}}(r, x) - \mathcal{C}_{\ell_{\text{def},k}}^B(\mathcal{R}, x) \\ &= \sum_{j=0}^J \bar{c}_j(a_j(x), z) 1_{j \in R_k(x)} - \sum_{i=0}^{k-1} \bar{c}_{[i]_{\bar{c}^*}}^*(a_{[i]_{\bar{c}^*}}(x), z) \\ &= \sum_{j=0}^J \bar{c}_j(a_j(x), z) 1_{j \in R_k(x)} - \sum_{i=0}^{k-1} \bar{c}_{[i]_{\bar{c}}}^{\uparrow}(a_{[i]_{\bar{c}}}^{\uparrow}(x), z) \\ &\quad + \left(\sum_{i=0}^{k-1} \bar{c}_{[i]_{\bar{c}}}^{\uparrow}(a_{[i]_{\bar{c}}}^{\uparrow}(x), z) - \sum_{i=0}^{k-1} \bar{c}_{[i]_{\bar{c}^*}}^*(a_{[i]_{\bar{c}^*}}(x), z) \right). \end{aligned} \quad (39)$$

Observing that:

$$\sum_{i=0}^{k-1} \bar{c}_{[i]_{\bar{c}}}^{\uparrow}(a_{[i]_{\bar{c}}}^{\uparrow}(x), z) - \sum_{i=0}^{k-1} \bar{c}_{[i]_{\bar{c}^*}}^*(a_{[i]_{\bar{c}^*}}(x), z) \leq \bar{c}_0(g(x), z) - \bar{c}_0^*(g(x), z), \quad (40)$$

we rewrite the first term using the conditional risks:

$$\sum_{j=0}^J \bar{c}_j(a_j(x), z) 1_{j \in R_k(x)} - \sum_{i=0}^{k-1} \bar{c}_{[i]_{\bar{c}}}^{\uparrow}(a_{[i]_{\bar{c}}}^{\uparrow}(x), z) = \mathcal{C}_{\ell_{\text{def},k}}(r, x) - \inf_{r \in \mathcal{R}} \mathcal{C}_{\ell_{\text{def},k}}(r, x). \quad (41)$$

Using the explicit formulation of the top- k deferral loss in terms of the indicator function $1_{j \notin R_k(x)}$ (Equation 16), we obtain:

$$\mathcal{C}_{\ell_{\text{def},k}}(r, x) - \inf_{r \in \mathcal{R}} \mathcal{C}_{\ell_{\text{def},k}}(r, x) = \sum_{j=0}^J \bar{\tau}_j(a(x), z) 1_{j \notin R_k(x)} - \inf_{r \in \mathcal{R}} \sum_{j=0}^J \bar{\tau}_j(a(x), z) 1_{j \notin R_k(x)}. \quad (42)$$

Using the change of variable $p_j = \frac{\bar{\tau}_j}{Q}$ with $Q = \sum_{j=0}^J \bar{\tau}_j$, it follows that:

$$\mathcal{C}_{\ell_{\text{def},k}}(r, x) - \inf_{r \in \mathcal{R}} \mathcal{C}_{\ell_{\text{def},k}}(r, x) = Q \left(\sum_{j=0}^J p_j 1_{j \notin R_k(x)} - \inf_{r \in \mathcal{R}} \sum_{j=0}^J p_j 1_{j \notin R_k(x)} \right). \quad (43)$$

Since the surrogate losses Φ_{01}^u are consistent with the top- k loss, we apply Lemma A.7:

$$\begin{aligned} \mathcal{C}_{\ell_{\text{def},k}}(r, x) - \inf_{r \in \mathcal{R}} \mathcal{C}_{\ell_{\text{def},k}}(r, x) &\leq Q \Gamma^u \left(\sum_{j=0}^J p_j \Phi_{01}^u(r, x, j) - \inf_{r \in \mathcal{R}} \sum_{j=0}^J p_j \Phi_{01}^u(r, x, j) \right) \\ &= Q \Gamma^u \left(\frac{1}{Q} \left[\mathcal{C}_{\Phi_{\text{def},k}}(r, x) - \inf_{r \in \mathcal{R}} \mathcal{C}_{\Phi_{\text{def},k}}(r, x) \right] \right). \end{aligned} \quad (44)$$

Incorporating Equation (40), we obtain:

$$\Delta \mathcal{C}_{\text{def},k}(r, x) \leq Q \Gamma^u \left(\frac{1}{Q} \left[\mathcal{C}_{\Phi_{\text{def},k}}(r, x) - \inf_{r \in \mathcal{R}} \mathcal{C}_{\Phi_{\text{def},k}}(r, x) \right] \right) + \bar{c}_0(g(x), z) - \bar{c}_0^*(g(x), z). \quad (45)$$

Taking expectations and applying Jensen's inequality for the concave function Γ^u yields:

$$\begin{aligned} \mathcal{E}_{\ell_{\text{def},k}}(g, r) - \mathcal{E}_{\ell_{\text{def},k}}^B(\mathcal{G}, \mathcal{R}) - \mathcal{U}_{\ell_{\text{def},k}}(\mathcal{G}, \mathcal{R}) &\leq \tilde{\Gamma}^u \left(\mathcal{E}_{\Phi_{\text{def},k}}(r) - \mathcal{E}_{\Phi_{\text{def},k}}^*(\mathcal{R}) - \mathcal{U}_{\Phi_{\text{def},k}}(\mathcal{R}) \right) \\ &+ \mathbb{E}_x \left[\bar{c}_0(g(x), z) - \inf_{g \in \mathcal{G}} \bar{c}_0(g(x), z) \right], \end{aligned}$$

where $\tilde{\Gamma}^u(v) = Q \Gamma^u(v/Q)$.

For the comp-sum surrogates, Mao et al. (2023b) derived tight transformation. Let $\Gamma^u(v) = \mathcal{W}^{-1}(v)^u$ an inverse transformation, then

$$\mathcal{T}(v)^u = \begin{cases} \frac{2^{1-v}}{1-v} \left[1 - \left(\frac{(1+v)^{\frac{2-v}{2}} + (1-v)^{\frac{2-v}{2}}}{2} \right)^{2-v} \right] & u \in [0, 1) \\ \frac{1+v}{2} \log[1+v] + \frac{1-v}{2} \log[1-v] & u = 1 \\ \frac{1}{(v-1)n^{v-1}} \left[\left(\frac{(1+v)^{\frac{2-v}{2}} + (1-v)^{\frac{2-v}{2}}}{2} \right)^{2-v} - 1 \right] & u \in (1, 2) \\ \frac{1}{(v-1)n^{v-1}} v & u \in [2, +\infty). \end{cases} \quad (46)$$

Therefore, if we specify $u = 1$ (log-softmax surrogate), we have the concave function $\Gamma^1(v) = \mathcal{W}^{-1}(v)^1$.

We have shown the consistency of our novel formulation. \square

A.11 Proof Lemma 4.8

Lemma 4.8 (Bayes-Optimal Rejector Set with Bayes-Optimal Cardinality). *Let $x \in \mathcal{X}$ and the learned rejector set $\hat{R}_k(x)$. Define the optimal cardinality as:*

$$s^B(x) = \arg \min_{v \in \mathcal{A}} \mathbb{E}_{z|x} \left[\ell_{\text{car}} \left(\hat{R}_{v+1}(x), v, a(x), z \right) \right],$$

where $\hat{R}_{v+1}(x)$ is a rejector set of size $v + 1$. Then, the Bayes-optimal rejector set $\hat{R}_{s^B(x)+1}(x)$ selects exactly the $s^B(x) + 1$ agents with the lowest Bayes-optimal expected costs:

$$\hat{R}_{s^B(x)+1}(x) = \hat{R}_k(x) \Big|_{k=s^B(x)+1}.$$

Proof. Recall first the Bayes-optimal rejector set:

$$R_k^B(x) = \arg \min_{\substack{R_k(x) \subseteq \mathcal{A} \\ |R_k(x)|=k}} \sum_{j \in R_k(x)} \bar{c}_j^*(a_j(x), z), \quad (47)$$

which selects those k agents in \mathcal{A} that minimize the sum of the optimal expected costs \bar{c}_j^* .

Next, define the *cardinality loss* ℓ_{car} and its conditional risk:

$$\mathcal{C}_{\ell_{\text{car}}}(s, x) = \mathbb{E}_{z|x} \left[\ell_{\text{car}}(R_{s(x)+1}(x), s(x), a(x), z) \right], \quad (48)$$

where $s(x) \in \mathcal{A}$ is a *selector* that assigns a number of agents $s(x) + 1$ to each input x . The corresponding Bayes-optimal conditional risk over all selectors $s \in \mathcal{S}$ is

$$\mathcal{C}_{\ell_{\text{car}}}^B(\mathcal{S}, x) = \min_{v \in \mathcal{A}} \mathbb{E}_{z|x} \left[\ell_{\text{car}}(R_{v+1}(x), v, a(x), z) \right]. \quad (49)$$

As a result, the *Bayes-optimal selector* $s^B(x)$ is exactly the function that solves

$$s^B(x) = \arg \min_{v \in \mathcal{A}} \mathbb{E}_{z|x} \left[\ell_{\text{car}}(R_{v+1}(x), v, a(x), z) \right], \quad (50)$$

Intuitively, for every x , we pick whichever cardinality $v + 1$ leads to the lowest conditional risk under ℓ_{car} .

Then, taking the top- $(s^B(x) + 1)$ agents leads to the following Bayes-optimal rejector set:

$$R_{s^B(x)+1}^B(x) = R_k^B(x) \Big|_{k=s^B(x)+1} \quad (51)$$

□

A.12 Choice of the metric d

The choice of the metric d in the cardinality loss depends on the application-specific objectives.

Classification Metrics for Cardinality Loss. In classification, common choices include:

- **Top- k Loss** A binary penalty is incurred when the true label y is not present in the prediction set:

$$d_{\text{top-}k}(R_{v+1}(x), v, a(x), y) = 1_{y \notin \{a_{[0]}(x), \dots, a_{[v]}(x)\}}.$$

- **Weighted Voting Loss.** Each agent is weighted according to a reliability score, typically derived from a softmax over the rejector scores $r(x, \cdot)$. The predicted label is obtained via weighted voting:

$$\hat{y} = \arg \max_{y \in \mathcal{Y}} \sum_{j \in R_{v+1}(x)} w_j \cdot 1_{a_j(x)=y}, \quad \text{with } w_j = \hat{p}(x, j) = \frac{\exp(r(x, j))}{\sum_{j'} \exp(r(x, j'))}.$$

The loss is defined as:

$$d_{\text{w-vl}}(R_{v+1}(x), v, a(x), y) = 1_{y \neq \hat{y}}.$$

- **Majority Voting Loss.** All agents contribute equally, and the predicted label is chosen by majority vote:

$$\hat{y} = \arg \max_{y \in \mathcal{Y}} \sum_{j \in R_{v+1}(x)} 1_{a_j(x)=y},$$

with the corresponding loss:

$$d_{\text{maj}}(R_{v+1}(x), v, a(x), y) = 1_{y \neq \hat{y}}.$$

Regression Metrics for Cardinality Loss. Let $\ell_{\text{reg}}(t, \hat{t}) \in \mathbb{R}^+$ denote a base regression loss (e.g., squared error or smooth L1). Common choices include:

- **Minimum Cost (Best Expert) Loss.** The error is measured using the prediction from the best-performing agent in the rejector set:

$$d_{\text{min}}(R_{v+1}(x), v, a(x), t) = \min_{j \in R_{v+1}(x)} \ell_{\text{reg}}(a_j(x), t).$$

- **Weighted Average Prediction Loss.** Each agent is assigned a reliability weight based on a softmax over rejector scores $r(x, \cdot)$. The predicted output is a weighted average of agent predictions:

$$\hat{t} = \sum_{j \in R_{v+1}(x)} w_j \cdot a_j(x), \quad \text{with } w_j = \frac{\exp(r(x, j))}{\sum_{j'} \exp(r(x, j'))},$$

and the loss is computed as:

$$d_{\text{w-avg}}(R_{v+1}(x), v, a(x), t) = \ell_{\text{reg}}(\hat{t}, t).$$

- **Uniform Average Prediction Loss.** Each agent in the rejector set contributes equally, and the final prediction is a simple average:

$$\hat{t} = \frac{1}{v+1} \sum_{j \in R_{v+1}(x)} a_j(x), \quad d_{\text{avg}}(R_{v+1}(x), v, a(x), t) = \ell_{\text{reg}}(\hat{t}, t).$$

A.13 Experiments

We compare our proposed *Top-k* and *Top-k(x)* L2D approaches against prior work (Narasimhan et al., 2022; Mao et al., 2023a, 2024), as well as against random and oracle (optimal) baselines.

A.13.1 Datasets

CIFAR-100. CIFAR-100 is a widely used image classification benchmark consisting of 60,000 color images of size 32×32 , evenly distributed across 100 fine-grained object categories (Krizhevsky, 2009). Each class contains 600 examples, with 50,000 images for training and 10,000 for testing. The large number of visually similar categories makes this dataset a challenging benchmark for evaluating multi-agent decision systems. We follow the standard split and apply dataset-specific normalization.

SVHN. The Street View House Numbers (SVHN) dataset (Goodfellow et al., 2014) is a digit classification benchmark composed of over 600,000 RGB images of 32×32 pixels, extracted from real-world street scenes (non-commercial use only). It contains significant variability in digit scale, orientation, and background clutter. We use the standard split: 73,257 training and 26,032 test images.

California Housing. The California Housing dataset (Kelley Pace and Barry, 1997) is a regression benchmark based on the 1990 U.S. Census (CCO). It contains 20,640 instances, each representing a geographical block in California and described by eight real-valued features (e.g., median income, average occupancy). The target is the median house value in each block, measured in hundreds of thousands of dollars. We standardize all features and use an 80/20 train-test split.

A.13.2 Metrics

For classification tasks, we report accuracy under three evaluation rules. The *Top-k Accuracy* is defined as $\text{Acc}_{\text{top-}k} = \mathbb{E}_x[1 - d_{\text{top-}k}(x)]$, where the prediction is deemed correct if the true label y is included in the outputs of the queried agents. The *Weighted Voting Accuracy* is given by $\text{Acc}_{\text{w-vl}} = \mathbb{E}_x[1 - d_{\text{w-vl}}(x)]$, where agent predictions are aggregated via softmax-weighted voting. Finally, the *Majority Voting Accuracy* is defined as $\text{Acc}_{\text{maj}} = \mathbb{E}_x[1 - d_{\text{maj}}(x)]$, where all agents in the rejector set contribute equally.

For regression tasks, we report RMSE under three aggregation strategies. The *Minimum Cost RMSE* is defined as $\text{RMSE}_{\text{min}} = \mathbb{E}_x[d_{\text{min}}(x)]$, corresponding to the prediction from the best-performing agent. The *Weighted Average Prediction RMSE* is given by $\text{RMSE}_{\text{w-avg}} = \mathbb{E}_x[d_{\text{w-avg}}(x)]$, using a softmax-weighted average of predictions. The *Uniform Average Prediction RMSE* is computed as $\text{RMSE}_{\text{avg}} = \mathbb{E}_x[d_{\text{avg}}(x)]$, using the unweighted mean of agent predictions.

In addition to performance, we also report two resource-sensitive metrics. The *expected budget* is defined as $\bar{\beta} = \mathbb{E}_x \left[\sum_{j=0}^{k-1} \beta_{[j]_{\hat{r}}} \right]$, where β_j denotes the consultation cost of agent j , and $[j]_{\hat{r}}$ is the index of the j -th ranked agent by the learned rejector \hat{r} . The *expected number of queried agents* is given by $\bar{k} = \mathbb{E}_x[|R_k(x)|]$, where k is fixed for Top- k L2D and varies with x in the adaptive Top- $k(x)$ L2D setting. Additional implementation and evaluation details are provided in Appendix A.12.

A.13.3 General Settings for Top- k and Top- $k(x)$ L2D

For each dataset, we configure a pool of six agents with a predefined consultation cost vector $\beta = (0, 0.05, 0.045, 0.040, 0.035, 0.03)$ and uniform scaling factors $\alpha_j = 1$, resulting in the agent index set $\mathcal{A} = \{0, 1, \dots, 5\}$. While the exact cost values are not critical to the Learning-to-Defer framework, they are chosen to simulate realistic deployment scenarios in which agents incur different operational costs (Madras et al., 2018; Mozannar and Sontag, 2020; Verma et al., 2022). This heterogeneity reflects systems composed of lightweight and heavyweight models, or a mixture of automated and human decision-makers with varying accessibility. The allocation policy is trained to account for both the predictive accuracy and consultation cost of each agent, thereby optimizing the overall cost-performance trade-off. For surrogates, we use the log-softmax loss $\Phi_{01}^{u=1}(r, x, j) = -\log \left(\frac{e^{r(x,j)}}{\sum_{j' \in \mathcal{A}} e^{r(x,j')}} \right)$ as our multiclass classification surrogate.

To assess the sensitivity of the selector and its impact on agent cardinality, we conduct experiments using multiple instantiations of the metric d ; detailed formulations are provided in

Section A.13.2. We additionally report results across a sweep of hyperparameters $\lambda \in \{1 \times 10^{-9}, 0.01, 0.05, 0.25, 0.5, 1, 1.5, \dots, 6.5\}$, which directly influence the learned number of agents $k = k(x)$. We choose to define the function $\xi(\cdot)$ as a linear function $\xi(v) = v$.

A.13.4 Reproducibility

All scripts and configurations are publicly available to facilitate reproducibility. We report both the mean and variance across four independent runs, with a fixed agent distribution. For random policies, results are averaged over fifty runs. All plots include error bars representing the mean and one standard deviation. Dataset-specific variability and additional implementation details are provided in the corresponding dataset sections.

A.14 Resources

All experiments were conducted on an internal cluster using an NVIDIA A100 GPU with 40 GB of VRAM. For Top- $k(x)$ L2D, the average GPU memory usage was approximately 7.2 GB for SVHN, 7.0 GB for CIFAR-100, and 6.8 GB for California Housing. In comparison, Top- k L2D required less memory: 2.0 GB for both SVHN and CIFAR-100, and 1.41 GB for California Housing.

A.14.1 Results on California Housing.

Agent setting. We construct a pool of 6 regression agents, each trained on a predefined, spatially localized subset of the California Housing dataset. To simulate domain specialization, each agent is associated with a specific geographical region of California, reflecting scenarios in which real estate professionals possess localized expertise. The training regions are partially overlapping to introduce heterogeneity and ensure that no single agent has access to all regions, thereby creating a realistic setting for deferral and expert allocation.

We train each agent using a multilayer perceptron (MLP) for 30 epochs with a batch size of 256, a learning rate of 1×10^{-3} , optimized using Adam. Model selection is based on the checkpoint achieving the lowest RMSE on the agent’s corresponding validation subset. We report the RMSE on the California validation set in table 1.

Agent	0	1	2	3	4	5
RMSE $\times 100$	21.97	15.72	31.81	16.20	27.06	40.26

Table 1: RMSE $\times 100$ of each agent on the California validation set.

Top- k L2D. We train a two-layer MLP following Algorithm 1. The rejector is trained for 100 epochs with a batch size of 256, a learning rate of 5×10^{-4} , using the Adam optimizer and a cosine learning rate scheduler. We select the checkpoint that achieves the lowest Top- k surrogate loss on the validation set, yielding the final rejector \hat{r} . We report Top- k L2D performance for each fixed value $k \in \mathcal{A}$.

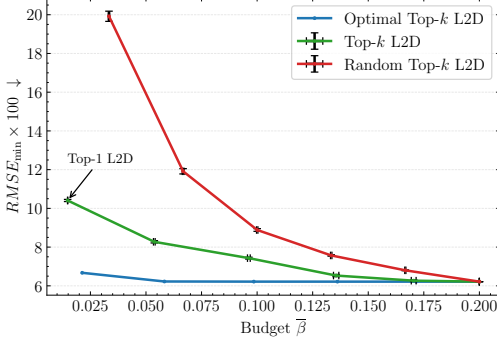
Top- $k(x)$ L2D. We train the selector using the same two-layer MLP architecture, following Algorithm 2. The selector is also trained for 100 epochs with a batch size of 256, a learning rate of 5×10^{-4} , using Adam and cosine scheduling. We conduct additional experiments using various instantiations of the metric d , as detailed in Section A.13.2.

Performance Comparison. Figures 5, compare Top- k and Top- $k(x)$ L2D across multiple evaluation metrics and budget regimes. Top- k L2D consistently outperforms random baselines and closely approaches the oracle (optimal) strategy under the RMSE_{min} metric, validating the benefit of using different agents (Table 1).

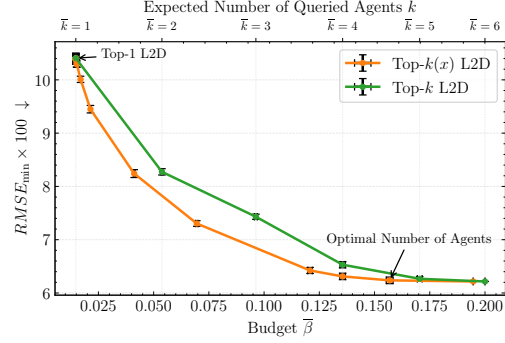
Specifically, in Figure 5b, Top- $k(x)$ achieves near-optimal performance (6.23) with a budget of $\bar{\beta} = 0.156$ and an expected number of agents $\bar{k} = 4.77$, whereas Top- k requires a full budget of $\bar{\beta} = 0.2$ and $\bar{k} = 6$ to reach comparable performance (6.21). This highlights the ability of Top- $k(x)$

Figure 5: Results on the California dataset comparing Top- k and Top- $k(x)$ L2D across four evaluation metrics. Top- $k(x)$ consistently achieves superior performance across all trade-offs.

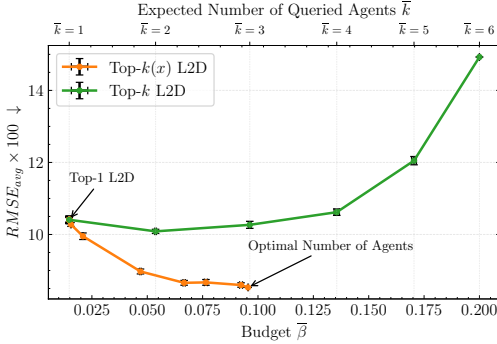
(a) Comparison with Random and Optimal Baselines: We compare Top- k L2D against random and oracle baselines using the RMSE_{\min} metric defined in Section A.13.2. Our method consistently outperforms both baselines and extends the Top-1 L2D formulation introduced by Mao et al. (2024).



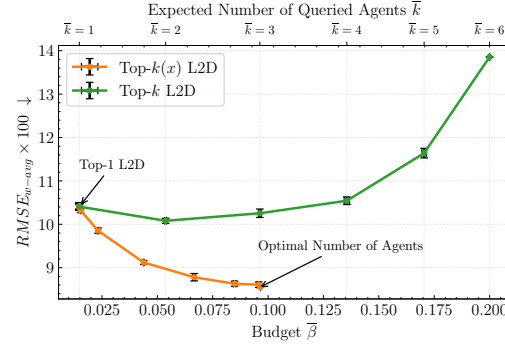
(b) Comparison of Top- k L2D and Top- $k(x)$ L2D under RMSE_{\min} metric. We report the RMSE_{\min} metric, along with the budget and the expected number of queried agents. Across all budgets, Top- $k(x)$ consistently outperforms Top- k L2D by achieving lower error with fewer agents and reduced cost.



(c) Comparison of Top- k L2D and Top- $k(x)$ L2D under RMSE_{avg} metric.



(d) Comparison of Top- k L2D and Top- $k(x)$ L2D under $\text{RMSE}_{w\text{-avg}}$ metric.



to allocate resources more efficiently by querying only the necessary number of agents, in contrast to Top- k , which often over-allocates costly or redundant agents.

Figures 5c and 5d evaluate Top- k and Top- $k(x)$ L2D under more restrictive metrics, where performance is not necessarily monotonic with respect to the number of agents. In such cases, querying too many or overly costly agents may degrade overall performance. Top- $k(x)$ L2D demonstrates clear advantages by carefully selecting the number of consulted agents. In both settings, it achieves optimal performance with a budget of only $\beta = 0.095$, whereas Top- k L2D fails to reach this level. For example, in Figure 5c, Top- $k(x)$ achieves $\text{RMSE}_{\text{avg}} = 8.53$, compared to $\text{RMSE}_{\text{avg}} = 10.08$ for Top- k . Similar trends are observed under the weighted average metric (Figure 5d), where Top- $k(x)$ again outperforms Top- k , suggesting that incorporating rejector-derived weights w_j is an effective strategy.

A.14.2 Results on SVHN

Agent setting. We construct a pool of 6 convolutional neural networks (CNNs), each trained on a randomly sampled, partially overlapping subset of the SVHN dataset (20%). This setup simulates realistic settings where agents are trained on distinct data partitions due to privacy constraints or institutional data siloing. As a result, the agents exhibit heterogeneous predictive capabilities and error patterns.

Each agent is trained for 3 epochs using the Adam optimizer (Kingma and Ba, 2017), with a batch size of 64 and a learning rate of 1×10^{-3} . Model selection is performed based on the lowest loss on each agent’s respective validation subset. The table 2 below reports the classification accuracy of each trained agent, evaluated on a common held-out validation set:

Agent	0	1	2	3	4	5
Accuracy (%)	63.51	55.53	61.56	62.60	66.66	64.26

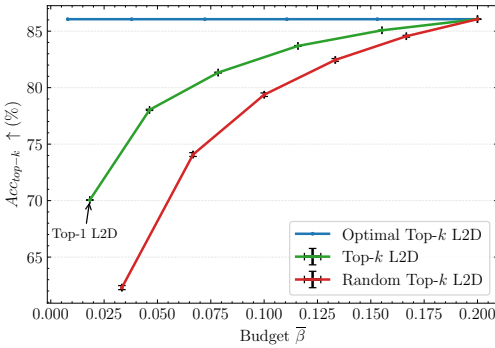
Table 2: Accuracy of each agent on the SVHN validation set.

Top- k L2D. We train the rejector using a ResNet-4 architecture (He et al., 2015), following Algorithm 1. The model is trained for 50 epochs with a batch size of 256 and an initial learning rate of 1×10^{-2} , scheduled via cosine annealing. Optimization is performed using the Adam optimizer. We select the checkpoint that minimizes the Top- k surrogate loss on the validation set, yielding the final rejector \hat{r} . We report Top- k L2D performance for each fixed value $k \in \mathcal{A}$.

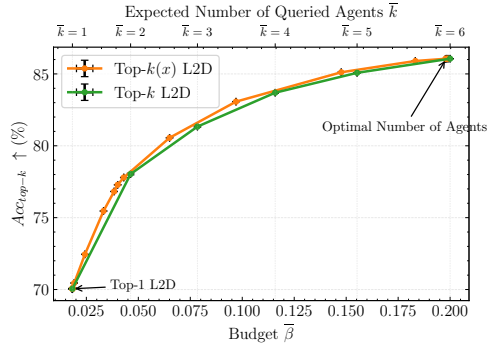
Top- $k(x)$ L2D. We reuse the trained rejector \hat{r} and follow Algorithm 2 to train a cardinality selector $s \in \mathcal{S}$. The selector is composed of a CLIP-based feature extractor (Radford et al., 2021) and a lightweight classification head. It is trained for 10 epochs with a batch size of 256, a learning rate of 1×10^{-3} , weight decay of 1×10^{-5} , and cosine learning rate scheduling. We use the AdamW optimizer (Loshchilov and Hutter, 2019) for optimization.

Figure 6: Comparison of Top- k and Top- $k(x)$ L2D across four accuracy metrics on SVHN. Top- $k(x)$ achieves better budget-accuracy trade-offs across all settings.

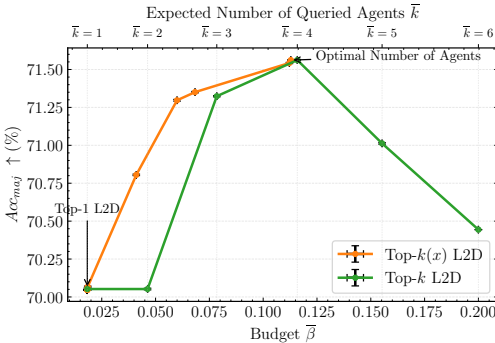
(a) Comparison with Random and Optimal baselines using $\text{Acc}_{\text{top-}k}$.



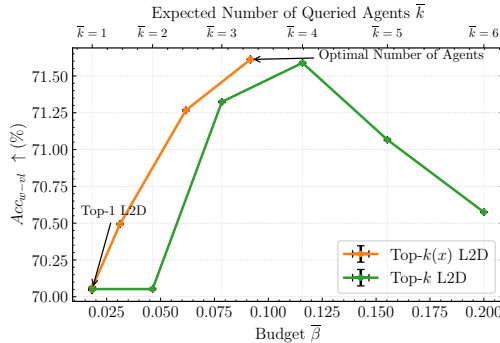
(b) Top- $k(x)$ vs. Top- k L2D on $\text{Acc}_{\text{top-}k}$.



(c) Performance under Acc_{maj} metric.



(d) Performance under Acc_{w-v1} metric.



Performance Comparison. Figure 6 compares our $Top-k$ and $Top-k(x)$ L2D approaches against prior work (Narasimhan et al., 2022; Mao et al., 2023a), as well as oracle and random baselines. As shown in Figure 6a, querying multiple agents significantly improves performance, with both of our methods surpassing the Top-1 L2D baselines (Narasimhan et al., 2022; Mao et al., 2023a). Moreover, our learned deferral strategies consistently outperform the random L2D baseline, underscoring the effectiveness of our allocation policy in routing queries to appropriate agents. In Figure 6b, $Top-k(x)$ L2D consistently outperforms $Top-k$ L2D, achieving better accuracy under the same budget constraints.

For more restrictive metrics, Figures 6c and 6d show that $Top-k(x)$ achieves notably stronger performance, particularly in the low-budget regime. For example, in Figure 6c, at a budget of $\bar{\beta} = 0.41$, $Top-k(x)$ attains $Acc_{maj} = 70.81$, compared to $Acc_{maj} = 70.05$ for $Top-k$. This performance gap widens further at smaller budgets. Both figures also highlight that querying too many agents may degrade accuracy due to the inclusion of low-quality predictions. In contrast, $Top-k(x)$ identifies a better trade-off, reaching up to $Acc_{maj} = 71.56$ under majority voting and $Acc_{w-vl} = 71.59$ with weighted voting. As in the California Housing experiment, weighted voting outperforms majority voting, suggesting that leveraging rejector-derived weights improves overall decision quality.

A.14.3 Results on CIFAR100.

Agent setting. We construct a pool of 6 agents. We train a main model (agent 0) using a ResNet-4 (He et al., 2015) for 50 epochs, a batch size of 256, the Adam Optimizer (Kingma and Ba, 2017) and select the checkpoints with the lower validation loss. We synthetically create 5 experts with strong overlapped knowledge. We assign experts to classes for which they have the probability to be correct reaching $p = 0.94$ and uniform in non-assigned classes. Typically, we assign 55 classes to each experts. We report in the table 3 the accuracy of each agents on the validation set.

Agent	0	1	2	3	4	5
Accuracy (%)	59.74	51.96	52.58	52.21	52.32	52.25

Table 3: Accuracy of each agent on the CIFAR100 validation set.

Top- k L2D. We train the rejector model using a ResNet-4 architecture (He et al., 2015), following the procedure described in Algorithm 1. The model is optimized using Adam with a batch size of 2048, an initial learning rate of 1×10^{-3} , and cosine annealing over 200 training epochs. We select the checkpoint that minimizes the Top- k surrogate loss on the validation set, resulting in the final rejector \hat{r} . We report Top- k L2D performance for each fixed value $k \in \mathcal{A}$.

Top- $k(x)$ L2D. We reuse the learned rejector \hat{r} and train a cardinality selector $s \in \mathcal{S}$ as described in Algorithm 2. The selector is composed of a CLIP-based feature extractor (Radford et al., 2021) and a lightweight classification head. It is trained using the AdamW optimizer (Loshchilov and Hutter, 2019) with a batch size of 128, a learning rate of 1×10^{-3} , weight decay of 1×10^{-5} , and cosine learning rate scheduling over 15 epochs. To evaluate performance under different decision rules, we conduct experiments using multiple instantiations of the metric d ; detailed definitions and evaluation protocols are provided in Section A.13.2.

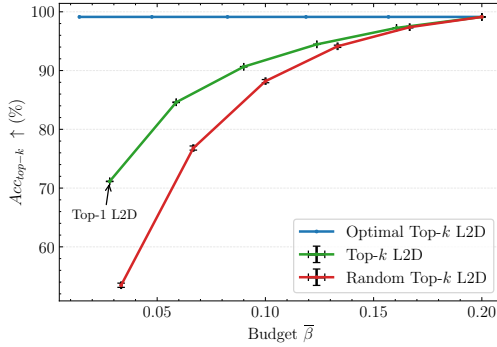
Performance Comparison. Figure 7b shows that Top- k L2D outperforms random query allocation, validating the benefit of learned deferral policies. As shown in Figure 7a, $Top-k(x)$ further improves performance over Top- k by adaptively selecting the number of agents per query. In Figures 7c and 7d, $Top-k(x)$ consistently yields higher accuracy across all budget levels, achieving significant gains over fixed- k strategies.

Notably, unlike in other datasets, querying additional agents in this setting does not degrade performance. This is due to the absence of low-quality agents: each agent predicts correctly with high probability (at least 94%) on its assigned class subset. As a result, aggregating predictions from multiple agents consistently improves accuracy.

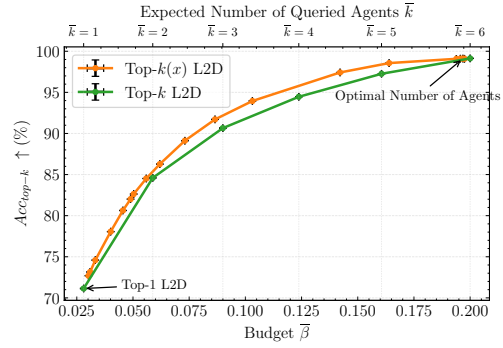
Nevertheless, Top- $k(x)$ remains advantageous due to the overlap between agents and their differing consultation costs. When several agents are likely to produce correct predictions, it is preferable to

Figure 7: Comparison of Top- k and Top- $k(x)$ L2D across four accuracy metrics on CIFAR100. Top- $k(x)$ achieves better budget-accuracy trade-offs across all settings.

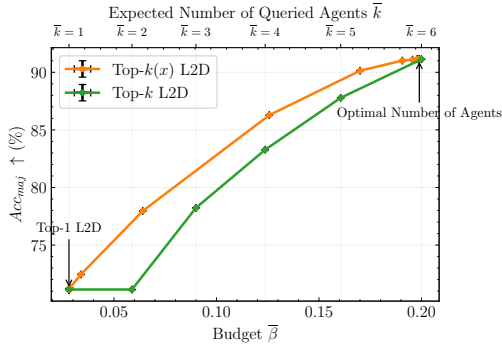
(a) Comparison with Random and Optimal baselines using Acc_{top-k} .



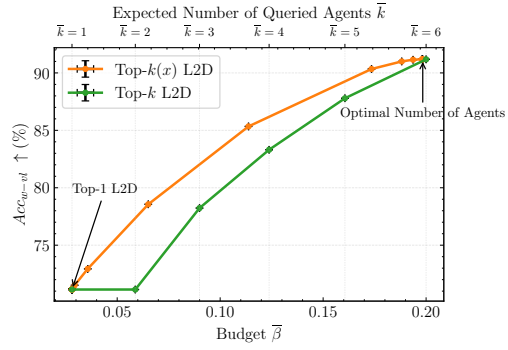
(b) Top- $k(x)$ vs. Top- k L2D on Acc_{top-k} .



(c) Performance under Acc_{maj} metric.



(d) Performance under Acc_{w-vl} metric.



defer to the less costly one. By exploiting this flexibility, Top- $k(x)$ achieves substantial performance improvements over Top- k L2D while also reducing the overall budget.